DOI: 10.1002/chem.201203387

Direct Evidence of Significantly Different Chemical Behavior and Excited-State Dynamics of 1,7- and 1,6-Regioisomers of Pyrrolidinyl-Substituted Perylene Diimide

Rajeev K. Dubey,* Marja Niemi, Kimmo Kaunisto, Alexander Efimov, Nikolai V. Tkachenko, and Helge Lemmetyinen[a]

Abstract: Novel bay-functionalized perylene diimides with additional substitution sites close to the perylene core have been prepared by the reaction between 1,7(6)-dibromoperylene diimide **6** (dibromo-PDI) and 2-(benzyloxymethyl)pyrrolidine **5**. Distinct differences in the chemical behaviors of the 1,7- and 1,6-regioisomers have been discerned. While the 1,6-dibromo-PDI produced the corresponding 1,6-bis-substituted derivative more efficiently, the 1,7-dibromo-PDI underwent predominant mono-debromination, yielding a mono-substituted PDI along with a small amount of the corresponding 1,7-bis-substituted compound. By varying the reaction conditions, a controlled stepwise bis-substitution of the bromo substituents was also achieved, allowing the direct synthesis of asymmetrical 1,6- and 1,7-PDIs. The compounds were isolated as individual regioisomers. Fullerene (C_{60}) was then covalently linked at the bay region of the newly prepared PDIs. In this way, two separate sets of perylene diimide–fullerene dyads, namely single-bridged (SB-1,7-PDI-C_{60} and SB-1,6-PDI-C_{60}) and double-bridged (DB-1,7-PDI-C_{60} and DB-1,6-PDI-C_{60}), were synthesized. The fullerene was intentionally attached at the bay region of the PDI to achieve close proximity of the two chromophores and to ensure an efficient photoinduced electron transfer. A detailed study of the photodynamics has revealed that photoinduced electron transfer from the perylene diimide chromophore to the fullerene occurs in all four dyads in polar benzonitrile, and also occurs in the single-bridged dyads in nonpolar toluene. The process was found to be substantially faster and more efficient in the dyads containing the 1,7-regioisomer, both for the singly- and double-bridged molecules. In the case of the single-bridged dyads, SB-1,7-PDI-C_{60} and SB-1,6-PDI-C_{60}, different relaxation pathways of their charge-separated states have been discovered. To the best of our knowledge, this is the first observation of photoinduced electron transfer in PDI-C_{60} dyads in a nonpolar medium.

Keywords: charge transfer · donor–acceptor systems · perylene diimide · photochemistry · regioisomers

Introduction

Perylene diimide (PDI) dyes have become key materials in a variety of technological applications owing to their peculiar properties such as intense absorption in the visible region, high fluorescence quantum yield, strong electron-accepting character, and excellent photochemical stability.[1] One of the crucial characteristics of these dyes, which greatly enhances their utility in comparison to other organic dyes, is the possibility of fine-tuning the molecular-level electronic and optical properties according to the requirements of various applications. As part of studies aimed at achieving this goal, several important advances have been made during the past decade. In this regard, functionalization of the "bay" region (1, 6, 7, and 12-positions) with either electron-donor or electron-acceptor groups has been the most effective and most applied approach to date. Therefore, driven by the demands of various applications, numerous bay-functionalized PDIs with interesting properties have been synthesized following this approach.[2] The last decade has witnessed their extensive utilization in numerous electronic and optical applications, including organic field-effect transistors (OFETs),[2a,b,3] organic light-emitting diodes (OLEDs),[4] logic gates,[5] organic solar cells,[6] photosensitizers,[7] sensors,[8] molecular wires,[9] and so forth. The strategy of bay substitution simultaneously gives rise to certain other key advantages. For example, it significantly improves the solubility of the dye by reducing π–π stacking, and also provides extra sites, in addition to the imido positions, for the attachment of other chromophores, which is essential for the construction of complex systems.[10] Therefore, the bay-functionalization approach is crucial for controlling the chemical structures and physical properties of PDI dyes.

[a] R. K. Dubey, M. Niemi, K. Kaunisto, A. Efimov, N. V. Tkachenko, H. Lemmetyinen
Department of Chemistry and Bioengineering
Tampere University of Technology
P.O. Box 541, 33101 Tampere (Finland)
Fax: (+358) 3-31152108
E-mail: rajeev.dubey@tut.fi

Supporting information for this article is available on the WWW under http://dx.doi.org/10.1002/chem.201203387.

The most elegant procedure for the preparation of bay-functionalized PDIs involves the use of 1,7-dibromoperylene diimide as the key intermediate due to facile exchange of the bromo substituents in the bay region with various nucleophiles. However, besides many advantages, the main issue of concern has been contamination with the corresponding 1,6-dibromo regioisomer, which is not only difficult to remove, but also difficult to detect by low-field (<400 MHz) ^{1}H NMR spectroscopy. This problem of contamination with around 25% of the 1,6-regioisomer remained unknown until the issue was first raised by Würthner et al. in 2004.[11] Scrutiny of the literature reveals that even after this unambiguous disclosure, the presence of the 1,6-regioisomer has been routinely ignored, and that a regioisomeric mixture of 1,7- and 1,6-disubstituted PDIs has been used in most studies in this field. The main reason for this negligence has presumably been a lack of awareness of any differences in the properties of the two regioisomers. Recent attention from researchers concerning this issue has resulted in a few reports on the separation, characterization, and respective optical and redox characteristics of some 1,7- and 1,6-disubstituted PDIs.[12] In most cases, however, the properties of the two regioisomers were found to be very similar.

Among the various bay-functionalized PDIs, 1,7-dipyrrolidinyl-PDI (so-called "green" PDI; Figure 1) has received particular interest because of its good electron-donating capability coupled with broad and strong absorption in the

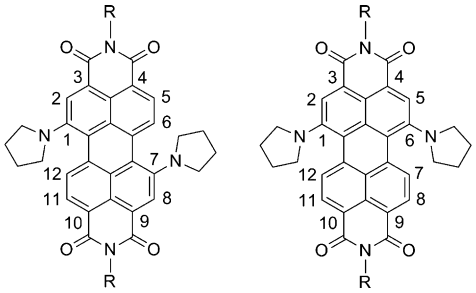

Figure 1. Chemical structures of 1,7- (left) and 1,6-regioisomers (right) of dipyrrolidinyl-substituted perylene diimide.

near-IR region, which helps to efficiently harvest solar energy.[13] Therefore, 1,7-dipyrrolidinyl-PDI has been the focus of many studies on solar-energy conversion, such as in light-harvesting antennas, artificial photosynthetic systems, and organic solar cells.[6,14] In addition, it has also attracted a great deal of attention in other important applications such as photoswitching, photochromism, and biochemistry.[15] However, as in the case of other 1,7-disubstituted PDIs, contamination with the 1,6-regioisomer has also been a problem with this dipyrrolidinyl derivative. In order to address this situation, we have recently separated 1,7- and 1,6-dipyrrolidinyl-PDIs (Figure 1) and have investigated their properties.[12a] In our expounded studies, both the optical and electrochemical properties of the 1,6-regioisomer were found to be highly depleted in comparison to those of the 1,7-regioisomer. The 1,7-dipyrrolidinyl-PDI is deep-green in color, whereas the corresponding 1,6-derivative is deep-blue.

In this report, we describe further comparative studies on the differences in the photoinduced properties of the 1,7- and 1,6-regioisomers in electron donor–acceptor (D–A) systems. In order to implement our thoughts, we designed two sets of dyads, namely, single-bridged dyads and double-bridged dyads, by the covalent attachment of fullerene to both of the separated 1,7- and 1,6-dipyrrolidinyl-PDIs through one and two linkers, respectively, at the bay region. The importance of the strategy of linking fullerene at the PDI core lies in the fact that it leads to close proximity of the donor and acceptor moieties, which is a crucial requirement in achieving efficient and rapid electron transfer.[16] Previously, fullerene has been linked to 1,7-dipyrrolidinyl-PDI through the imido position, which keeps the two moieties significantly apart from one another.[17] Consequently, the dyad demonstrated photoinduced electron transfer only in polar solvents. In nonpolar solvents, energy transfer governed the excited-state deactivation. In the present PDI-C_{60} dyads, with the moieties in close proximity, we expected an improved electron-transfer process, which was the second objective of this work. Various experimental techniques, including steady-state absorption and emission spectroscopies, picosecond pump-probe analysis, nanosecond flash-photolysis, differential pulse voltammetry, and NMR spectroscopy, have been employed to investigate in detail the photoinduced electron transfer in these dyads. This is the first report in which the performances of the two regioisomers in a donor–acceptor-based system have been examined and compared.

Results and Discussion

Synthesis and characterization

Synthesis of double-bridged dyads: The dyads (DB-1,7-PDI-C_{60} and DB-1,6-PDI-C_{60}) were prepared from a mixture of 1,7- and 1,6-regioisomers of dibromo-PDI **6** according to the route summarized in Schemes 1–4. This regioisomeric mixture **6** was synthesized according to the well-established procedure.[11,12a] The mixture was used for the further reactions without isolation of the two isomers. In order to synthesize these dyads, the first task was to select and synthesize a suitable pyrrolidine derivative that would readily react with dibromo-PDI **6** while also tolerating the harsh reaction conditions. For this purpose, we chose L-proline **1** as the starting compound and transformed it into 2-(benzyloxymethyl)pyrrolidine **5** in four straightforward steps, as depicted in Scheme 1. In the first step, the amino group of L-proline **1** was protected with a *tert*-butyloxy carbonyl (Boc) group to produce **2** in 90% yield. Subsequent reduction of the free carboxylic acid group with BH_3·THF gave 2-(hydroxymethyl)-*N*-Boc-pyrrolidine **3** in 99% yield. The third step was to protect the free hydroxyl group of **3** by reaction with benzyl bromide, which gave 2-(benzyloxymethyl)-*N*-Boc-pyrrol-

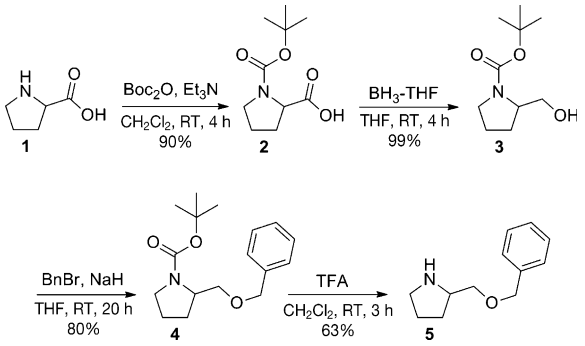

Scheme 1. Synthesis of 2-(benzyloxymethyl)pyrrolidine **5** from L-proline **1**; (Bn = benzyl).

idine **4** in 80% yield. Finally, the Boc protection was removed by treatment with trifluoroacetic acid (TFA) to produce 2-(benzyloxymethyl)pyrrolidine **5** in 63% yield. Of the many groups available for protecting hydroxyl groups, we selected the benzyloxy group because of its electron-donating nature and robustness towards the harsh reaction conditions. The electron-donating ability was highly desirable in order to enhance the reactivity of 2-(benzyloxymethyl)pyrrolidine **5** as a nucleophile.

The next task was to attach 2-(benzyloxymethyl)pyrrolidine **5** to the PDI core through substitution of the bromo substituents of the dibromo-PDI precursor **6** to obtain *N,N'*-dioctyl-1,7(6)-bis[2-(benzyloxymethyl)pyrrolidinyl]perylene diimide **9** (Scheme 2). Considering that the attachment of a functionalized pyrrolidine to a PDI core is apparently unprecedented, this was considered to pose the biggest challenge in the whole synthetic scheme. However, the reaction for attaching pyrrolidine at the bay positions is well established, and has been routinely used to synthesize dipyrrolidinyl-substituted PDI derivatives for over a decade.[2d] This reaction is performed by heating a solution of dibromo-PDI **6** in neat pyrrolidine at 55 °C for a day, in which the pyrrolidine serves as both reagent and solvent. Pyrrolidine can serve as the solvent for this reaction because it is a free-flowing liquid (density 0.852 g mL^{-1}) and readily dissolves dibromo-PDI **6**. In contrast to pyrrolidine itself, functionalized pyrrolidines are either solids or dense viscous liquids, thus necessitating the use of an external solvent. Consequently, in order to realize this reaction, all of the crucial parameters, such as solvent, amount of 2-(benzyloxymethyl)pyrrolidine **5**, temperature, and duration had to be identified and optimized.

As part of a systematic study aimed at meeting this objective, numerous reactions were tested under different conditions. The most informative results are summarized in Table 1 and the most successful reactions are shown in Scheme 2. Considering that dibromo-PDI **6** dissolves best in moderately polar solvents, we first tested the use of $CHCl_3$ containing an excess (840 mol%) of 2-(benzyloxymethyl)-pyrrolidine **5**. The reaction temperature was initially selected as 55 °C (Table 1, entry 1), based on the fact that the coupling between pyrrolidine and dibromoperylene diimide proceeds smoothly at this temperature. In the present case, however, even after prolonged heating, the bis-substituted product **9** was not obtained (Scheme 2). Instead, the reac-

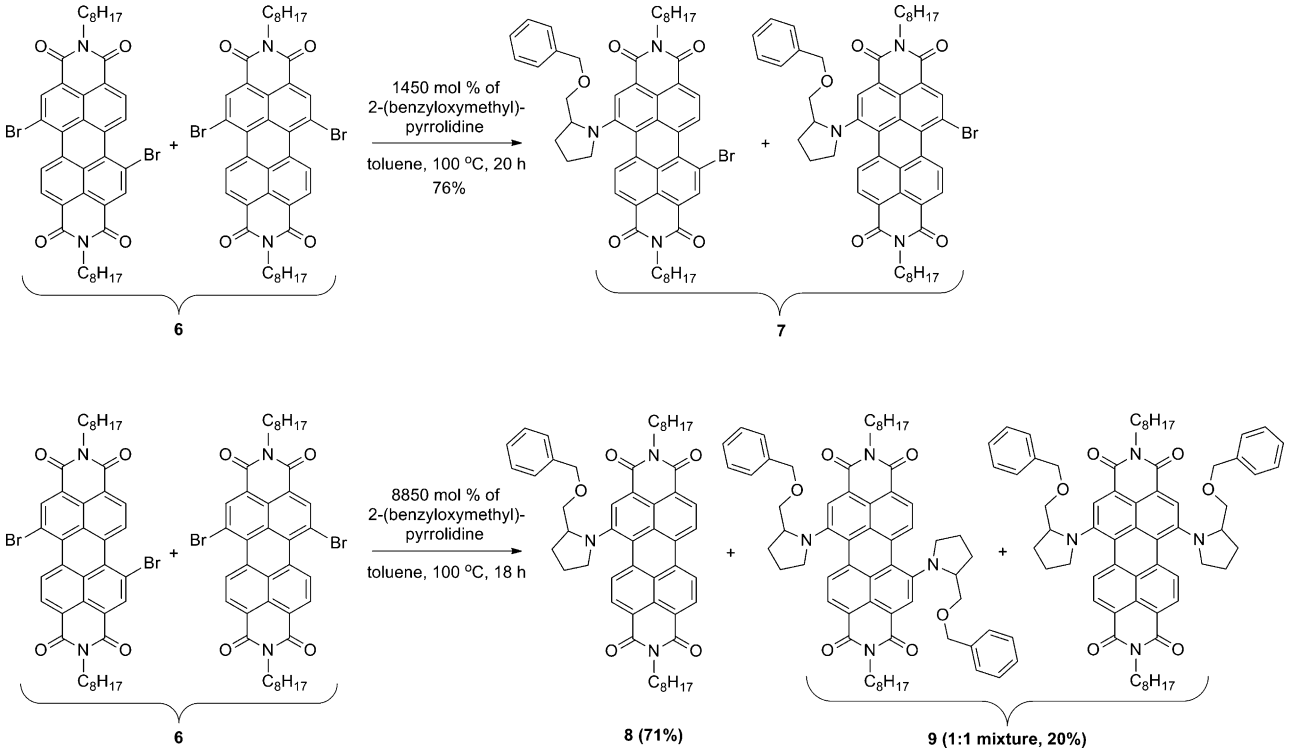

Scheme 2. Synthesis of 2-(benzyloxymethyl)pyrrolidinyl-functionalized perylene diimides (**7**, **8**, and **9**).

Table 1. Coupling reaction of 2-(benzyloxymethyl)pyrrolidine **5** and dibromoperylene diimide **6**.

Entry	Solvent[a]	**5**[b] [mol%]	*T* [°C]	*t* [h]	Yield **7** [%]	Yield **8** [%]	Yield **9** [%]	Yield **6** [%][c]
1	chloroform	840	55	24	10	–	–	80
2	toluene	840	90	24	50	–	–	46
3	toluene	1450	100	20	76	–	4	18
4	toluene	4000	100	21	5.7	72	10	–
5	toluene	8850	100	18	–	71	20	–
6	NMP	4000	100	20	4	43	8	–
7	NMP	8000	100	10	–	65	11	–
8	NMP	4000	100	5	50	23	10	–
9	NMP	1600	100	20	2	62	5	–
10	NMP	1600	90	20	30	34	4	–
11	NMP	9300	140	1	19	–[d]	–[d]	14

[a] Dibromoperylene diimide (**6**) was dissolved in the minimum possible volume of NMP by heating. [b] 2-(Benzyloxymethyl)pyrrolidine (**5**). [c] Recovered from the reaction. [d] *N,N′*-Dioctyl-1-bromo-7(6)-hydroxyperylene diimide was the main product.

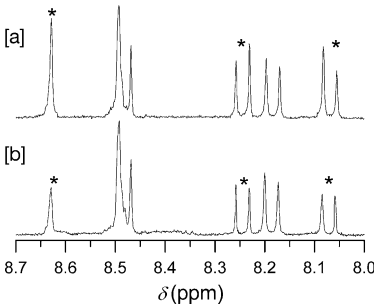

Figure 2. ^{1}H NMR spectra (300 MHz, $CDCl_3$, aromatic region) revealing the composition of 1,7- and 1,6-regioisomers in the bis-substituted product **9** obtained from the reaction carried out a) in toluene and b) in NMP. The signals corresponding to the 1,7-regioisomer are marked with asterisks.

tion yielded a small amount (ca. 10%) of the mono-substituted derivative **7**. Based on this result, we incrementally raised the reaction temperature, which provided accordingly increased yields of **7**. When the reaction was carried out in toluene at 100°C with 1450 mol% of 2-(benzyloxymethyl)-pyrrolidine **5**, the target bis-substituted product **9** was successfully obtained for the first time, although the yield was very low (4%, entry 3). This reaction, however, produced a high yield (76%) of the mono-substituted derivative **7**. Therefore, these reaction conditions can be used for the efficient synthesis of **7**, which serves as an important synthon for the synthesis of asymmetrically bay-substituted PDIs.

In the next step, with a view to enhance the yield of bis-substituted product **9**, we further increased the amount of **5**, which led to quite surprising results. When the reaction was carried out in the presence of 4000 mol% of 2-(benzyloxymethyl)pyrrolidine **5** (Table 1, entry 4), the mono-debrominated compound **8** was unexpectedly obtained as the major product in high yield (72%). At the same time, the desired bis-substituted product **9** was obtained as a minor product in just 10% yield. Separation of compounds **8** and **9** by column chromatography proved very difficult due to their similar mobilities. Ultimately, they were separated on HPTLC glass plates, eluting with $CHCl_3$/toluene (2:1). Most unexpectedly, ^{1}H NMR analysis of the greenish-blue bis-substituted product **9** clearly revealed the presence of 1,7- and 1,6-regioisomers in an approximately 1:1 ratio, based on the intensities of the characteristic signals of the PDI core protons (one singlet and two doublets) in the aromatic region (Figure 2a). Statistically, the amount of the 1,7-regioisomer in the product **9** was expected to be approximately three times higher than that of the corresponding 1,6-regioisomer, because the starting compound dibromo-PDI **6** was composed of 1,7- and 1,6-regioisomers in an approximately 3:1 ratio. Very similar results were obtained when the reaction was performed with an even larger excess (8850 mol%) of **5** (Table 1, entry 5). Again, the reaction yielded the unexpected mono-debrominated derivative **8** in a high yield of 71%. However, this time an improved yield (20%) of the desired bis-substituted product **9** was obtained, the 1,7- and 1,6-regioisomers of which were again found to be in a ratio of approximately 1:1. On the other hand, when the reaction time was shortened, the mono-substituted derivative **7** was obtained as the major product in high yield.

The abovementioned results clearly indicate a difference in the chemical behaviors of the 1,7- and 1,6-regioisomers. Evidently, in the presence of a large excess of 2-(benzyloxymethyl)pyrrolidine **5**, both the 1,7- and 1,6-regioisomers of dibromo-PDI **6** first undergo mono-substitution very smoothly to give *N,N′*-dioctyl-1-bromo-7(6)-[2-(benzyloxymethyl)pyrrolidinyl]perylene diimide **7** in high yield. At this stage, however, the major 1,7-regioisomer undergoes debromination to yield **8** more efficiently than the corresponding 1,6-regioisomer. Therefore, the reaction produces the mono-debrominated product **8** as the major product in a high yield of around 71% and the bis-substituted product **9** as a minor product, which comprises approximately equal amounts of the 1,7- and 1,6-isomers. These two regioisomers of the bis-substituted product **9** could not be separated due to their similar mobilities. Therefore, the 1:1 mixture of the two regioisomers was used as such for the next reaction.

We also evaluated performance of the reaction in basic solvents in the hope of obtaining a higher yield of the desired bis-substituted product **9** than that obtained in toluene (20%). We first tested *N,N′*-dimethyl acetamide (DMA) as the solvent, but no product was obtained even at high temperatures or after a prolonged reaction time. Subsequently, we carried out reactions in the more basic *N*-methyl-2-pyrrolidinone (NMP) under similar conditions, whereupon the mono-debrominated compound **8** was again obtained as the major product (ca. 60% yield) along with the desired bis-substituted product **9** as a minor product (ca. 10% yield; Table 1, entries 6 and 7). In this case, however, the bis-substituted product **9** consisted of an even higher proportion of the 1,6-regioisomer over that of the corresponding 1,7-regioisomer (Figure 2b). The reaction was also evaluated with a shorter duration (Table 1, entry 8), a lower proportion of **5** (Table 1, entry 9), and at a lower temperature (Table 1,

entry 10), but the yield of the bis-substituted product **9** was not improved. Finally, we also tried to perform the reaction at temperatures as high as 140 °C (entry 11). However, these extreme conditions favored oxidation of the dibromo-PDI to produce 1-bromo-7(6)-hydroxy-PDI, as revealed by MS analysis.

The present study revealed that a high temperature, of the order of 100 °C, is essential for efficient attachment of 2-(benzyloxymethyl)pyrrolidine **5** to the PDI core. In addition, the choice of solvent was found to be crucial for this reaction. The yield of the mono-substituted product **7** was drastically reduced when toluene was replaced with the more basic solvent NMP (Table 1, entries 3 and 9). Similarly, the yield of the bis-substituted product **9** was also found to be higher in toluene compared to that in NMP (Table 1, entries 5 and 7). This can be attributed to the higher basicity of NMP, which enhances the rate of debromination. Furthermore, the reaction is highly sensitive to changes in the amount of 2-(benzyloxymethyl)pyrrolidine **5** relative to dibromo-PDI **6**. In toluene, in the presence of a lower amount of **5** (ca. 1450 mol %), the reaction produces the mono-substituted compound **7** as the major product (Table 1, entry 3). However, in the presence of a larger excess of **5**, it yields the debrominated compound **8** as the major product (Table 1, entries 4 and 5).

Before further reactions could be attempted, both hydroxyl groups of compound **9** had to be unmasked by de-*O*-benzylation. This was successfully carried out with BBr_3 in dry CH_2Cl_2 at −78 °C, as illustrated in Scheme 3. The crude product was first purified by column chromatography (silica-100; $CHCl_3$) to afford a regioisomeric mixture of the desired molecules **10** and **11** in around 65 % yield. Subsequently, the 1,7-regioisomer **10** (dark green in color) and the corresponding 1,6-regioisomer **11** (dark blue in color) were successfully separated on HPTLC glass plates, eluting with $CHCl_3$. The separation of these regioisomers was verified by ^{1}H NMR spectroscopy.

In the penultimate step, the unmasked hydroxyl groups of compounds **10** and **11** were used for the attachment of malonate fragments by reaction with ethyl malonyl chloride to afford the corresponding PDIs **12** and **14** (Scheme 4). Finally, fullerene was double-linked to these PDIs (**12** and **14**) by a Bingel reaction in order to prepare the desired dyads DB-1,7-PDI-C_{60} (**13**) and DB-1,6-PDI-C_{60} (**15**), respectively.[18]

The dyads were initially purified by column chromatography on silica gel immediately after completion of the reactions. Since high purity of the dyads was crucial for the photophysical studies, they were additionally purified on HPTLC glass plates. ESI-MS and ^{1}H NMR spectroscopy provided unambiguous proof of the formation of the dyads. Detailed analysis of the substitution pattern on the fullerene could not be conducted because of insufficient quantities of the dyads, along with crowded and overlapped ^{13}C NMR signals and UV/Vis absorptions of the PDI and fullerene moieties. Presumably, both dyads were mixtures of fullerene regioisomers; however, we did not observe separate zones or inhomogeneities in the dyad fractions during HPTLC purification.

Synthesis of single-bridged dyads: The single-bridged dyads (SB-1,7-PDI-C_{60} **20** and SB-1,6-PDI-C_{60} **22**) were synthesized from *N*,*N*′-dioctyl-1-bromo-7(6)-[2-(benzyloxymethyl)-pyrrolidinyl]perylene diimide **7** according to the route summarized in Scheme 5. In the first step, a pyrrolidine group was attached to **7** by substitution of the bromo substituent to obtain **16** as a regioisomeric mixture in 64 % yield. The 1,7- and 1,6-regioisomers could not be separated chromatographically. Therefore, compound **16** was used as a mixture for the following reaction, in which deprotection of the hydroxyl group by using BBr_3 gave a mixture of **17** and **18** in high yield (99 %). The 1,7- and 1,6-regioisomers could then be successfully separated by column chromatography as individual regioisomerically pure *N*,*N*′-dioctyl-1-pyrrolidinyl-7-[2-(hydroxymethyl)pyrrolidinyl]perylene diimide **17** and *N*,*N*′-dioctyl-1-pyrrolidinyl-6-[2-(hydroxymethyl)pyrrolidinyl]perylene diimide **18**. In the following step, separate reactions of **17** and **18** with ethyl malonyl chloride provided the corresponding PDIs **19** and **21**, respectively, in high yields of about 95 %. Finally, fullerene was linked to the pendant malonate moieties of PDIs **19** and **21** by a Bingel reaction to furnish the corresponding dyads SB-1,7-PDI-C_{60} (**20**) and SB-1,6-PDI-C_{60} (**22**) in yields of 50 and 41 %, respectively.[18]

^{1}H NMR analysis: The aromatic regions of the ^{1}H NMR spectra of the double-bridged dyads DB-1,7-PDI-C_{60} and DB-1,6-PDI-C_{60} were compared with the spectra of respective ref-PDIs to analyze the effect of the fullerene on the PDI core protons (Figure 3). The information provided was

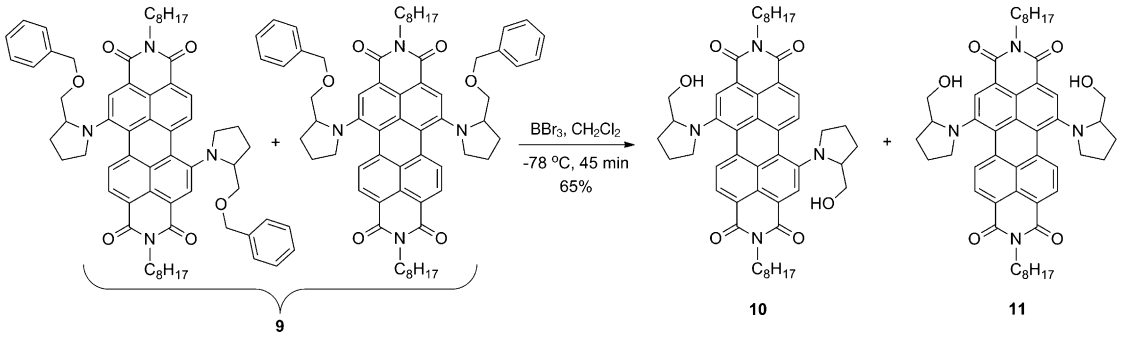

Scheme 3. Oxidative de-*O*-benzylation of **9** by BBr_3 to afford **10** and **11**.

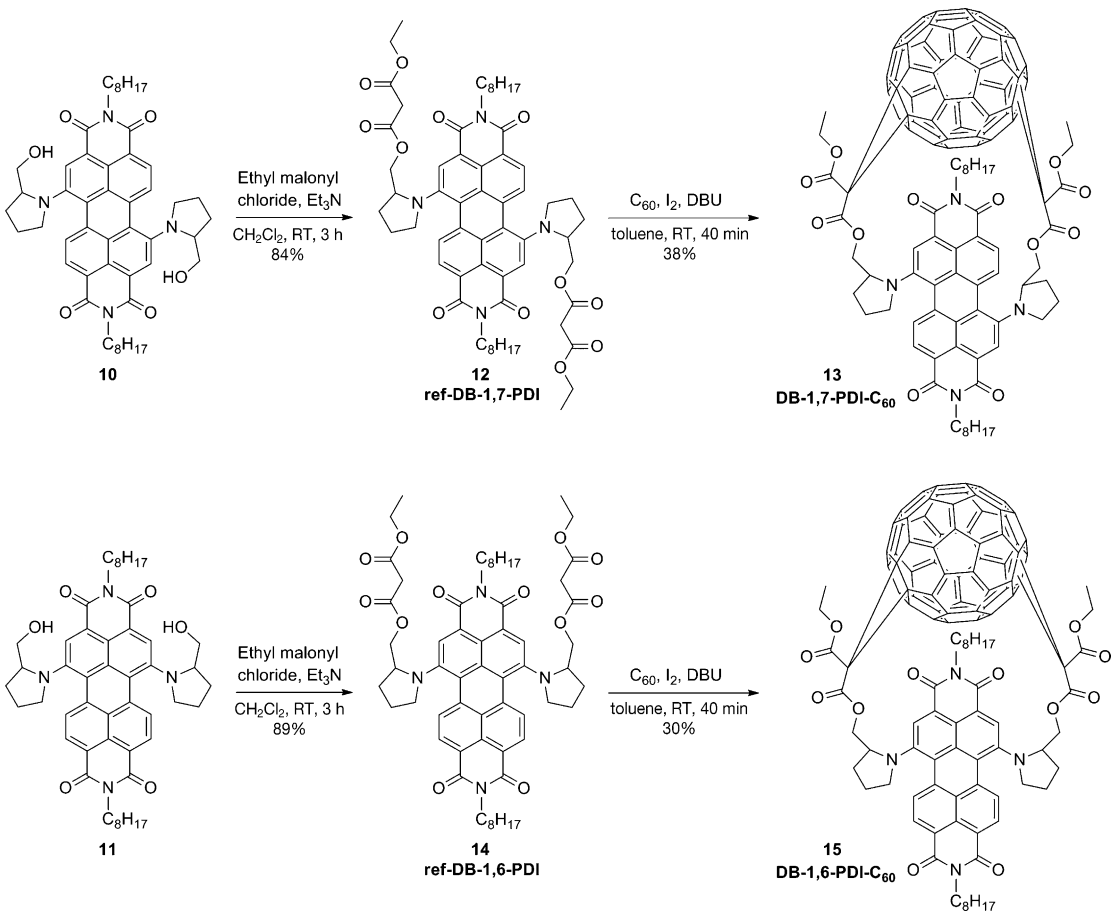

Scheme 4. Synthesis of double-bridged dyads; DB-1,7-PDI-C_{60} **13** and DB-1,6-PDI-C_{60} **15** (DBU = 1,8-Diazabicyclo[5.4.0]undec-7-ene).

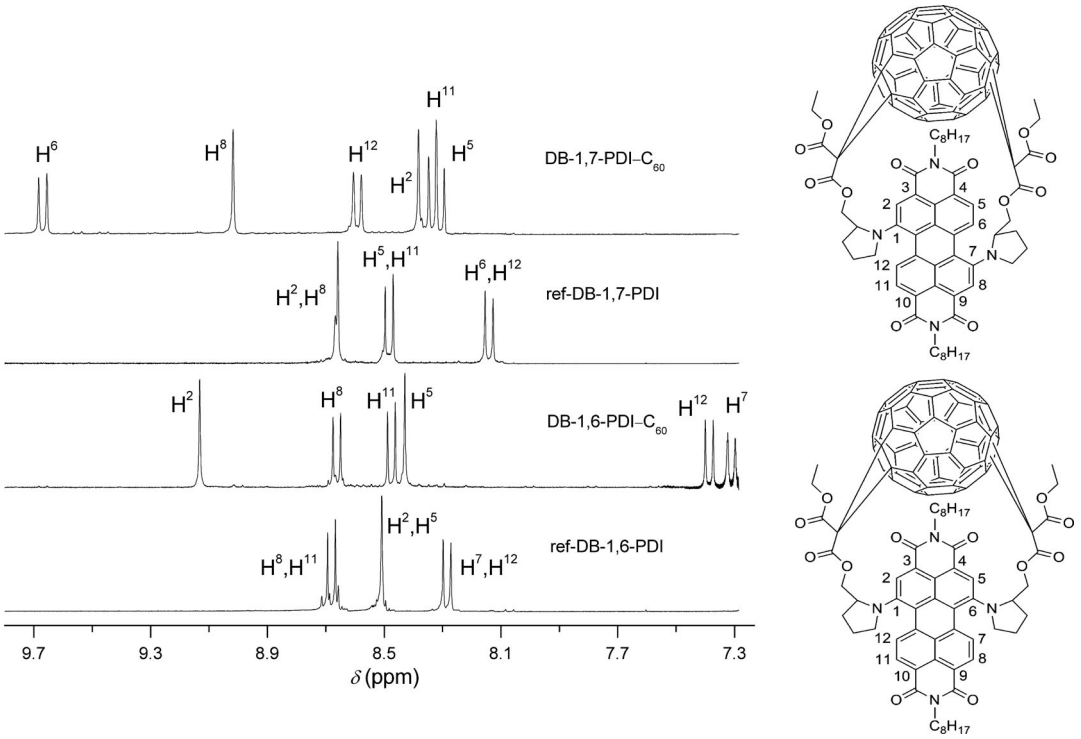

Figure 3. Comparison of ^{1}H NMR spectra of DB-1,7-PDI-C_{60} and DB-1,6-PDI-C_{60} with those of ref-DB-1,7-PDI and ref-DB-1,6-PDI, respectively.

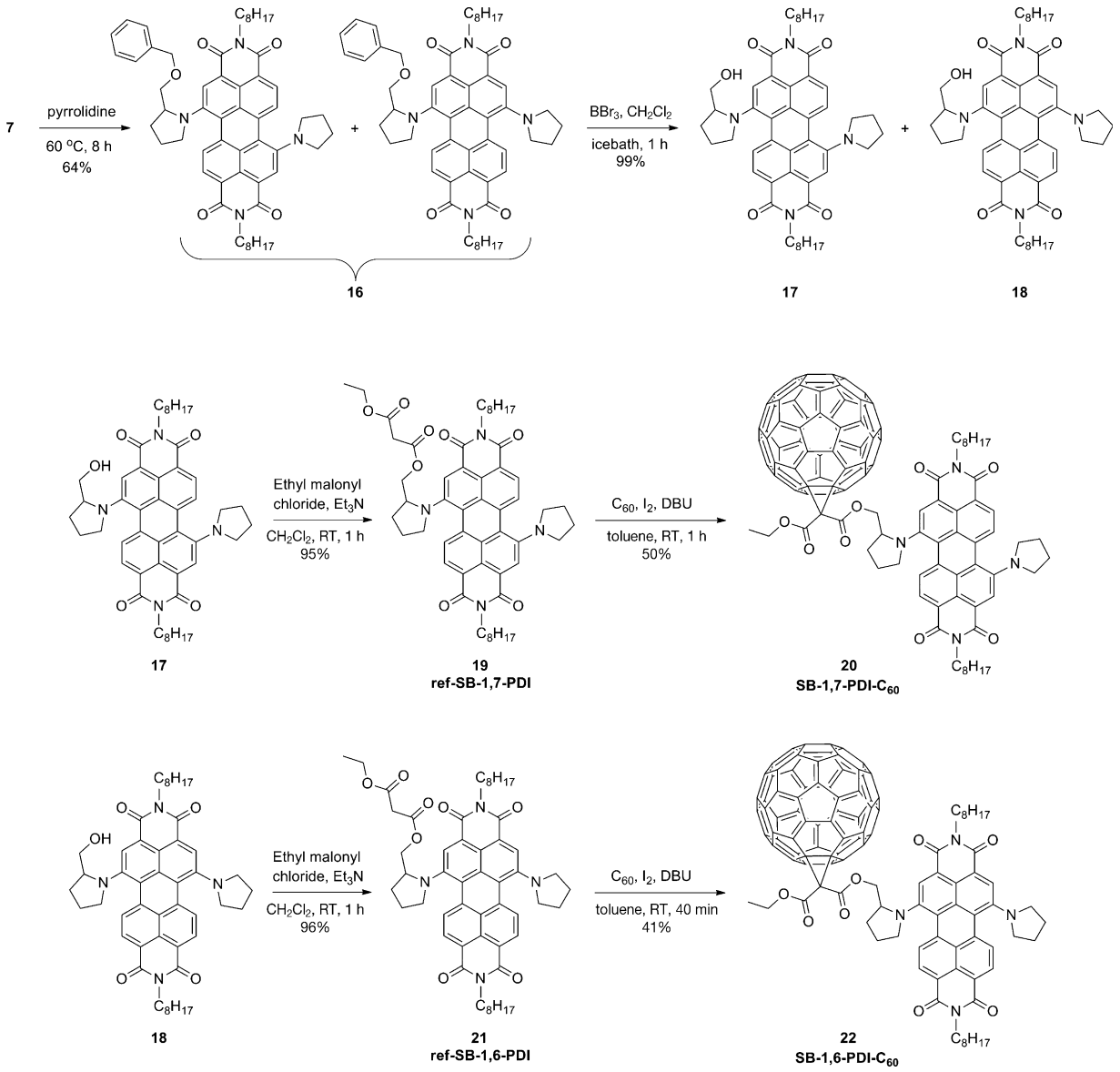

Scheme 5. Synthesis of single-bridged dyads; SB-1,7-PDI-C_{60} **20** and SB-1,6-PDI-C_{60} **22**.

used to make a preliminary assessment of the mutual orientation of the two interacting chromophores in these double-bridged dyads. The various signals were tentatively assigned to the protons of the dyads with the help of ^1H–^1H COSY measurements (Figures S1 and S2 in the Supporting Information). In both dyads, the attachment of fullerene resulted in significant shifts in the signals of nearly all of the PDI core protons, which clearly revealed the close proximity of the two chromophores. However, some interesting differences were also observed in the shift patterns between the two dyads. In DB-1,7-PDI-C_{60}, large downfield shifts of $\Delta\delta =$ 1.53 and 0.36 ppm were displayed by two protons (H^6 and H^8, respectively) due to the deshielding effect exerted by the π-electrons of C_{60}. In DB-1,6-PDI-C_{60}, on the other hand, three protons, namely H^2, H^7, and H^{12}, were most affected by the π-electrons of C_{60}. Of these, only one proton (H^2) displayed a downfield shift ($\Delta\delta = 0.63$ ppm). The other two protons, H^7 and H^{12}, experienced a shielding effect, which resulted in large upfield shifts of $\Delta\delta = 0.97$ and 0.90 ppm, respectively. These very clear differences in the shift patterns of the PDI core protons can be considered as indications of different orientations of C_{60} with respect to the PDI in these two double-bridged dyads. This difference in orientation can also be anticipated based on the different bay positions of the PDI moieties to which the linkers are appended in the two dyads. In the case of dyad DB-1,7-PDI-C_{60}, the linkers are appended at the 1- and 7-positions, which leads to better face-to-face orientation of the two chromophores. In the dyad DB-1,6-PDI-C_{60}, the 1- and 6-positions are located on the same side of the perylene core, resulting in orientation of the fullerene more towards the imide position.

The ^{1}H NMR spectra of the single-bridged dyads, SB-1,7-PDI-C_{60} and SB-1,6-PDI-C_{60}, were similarly analyzed. The effect of the fullerene moiety on the signals of the PDI core protons was also clearly observed in these dyads. However, in these single-bridged dyads, the shifts were significantly smaller than those observed for the double-bridged dyads. These observations clearly suggest that the PDI and fullerene moieties are in close proximity in both the doubly-and single-bridged dyads, although more so in the former than in the latter.

Electrochemical properties: Differential pulse voltammetric (DPV) studies were performed to compare the redox characteristics of the individual entities with those of the dyads to obtain a better understanding of the ground-state interaction between the two closely linked moieties.

The DPV results (Table 2) led us to two notable observations. Firstly, the 1,7- and 1,6-regioisomers exhibit pronounced differences in their oxidation characteristics, which reflect a clear difference in their electron-donating capabilities. The ref-SB-1,7-PDI exhibits significantly lower first and second oxidation potentials (+0.67 and +0.82 V) in comparison to those of ref-SB-1,6-PDI (+0.82 and +1.27 V). Similar differences were also observed in the case of ref-DB-1,7-PDI (+0.72 and +0.87 V) and its corresponding 1,6-regioisomer ref-DB-1,6-PDI (+0.93 and +1.34 V). Consequently, 1,7-substituted PDIs are better electron donors than the corresponding 1,6- derivatives. Moreover, among the single-bridged dyads, the energy of the charge-separated state was found to be lower for SB-1,7-PDI-C_{60} (1.20 eV) than for SB-1,6-PDI-C_{60} (1.35 eV). Similarly, among the double-bridged dyads, DB-1,7-PDI-C_{60} (1.51 eV) exhibited lower energy of the charge-separated state than DB-1,6-PDI-C_{60} (1.56 eV). Based on these observations, we could anticipate more efficient electron transfer in the dyads incorporating the 1,7-regioisomer as the donor in comparison to the corresponding dyads with the 1,6-regioisomer.

Table 2. Redox potentials (V vs. Ag/AgCl) of dyads and reference compounds obtained by DPV in PhCN.[a]

Compound	E_{1ox}	E_{2ox}	E_{1red}	E_{2red}	E_{CS} [eV][b]
ref-SB-1,7-PDI	+0.67	+0.82	−0.81	−0.99	–
SB-1,7-PDI-C_{60}	+0.69	+0.86	−0.51	−0.92[c]	1.20
ref-SB-C_{60}	+1.68	–	−0.50	−0.92	–
SB-1,6-PDI-C_{60}	+0.83	+1.30	−0.52	−0.93[c]	1.35
ref-SB-1,6-PDI	+0.82	+1.27	−0.81	−0.97	–
ref-DB-1,7-PDI	+0.72	+0.87	−0.79	−0.99	–
DB-1,7-PDI-C_{60}	+0.90	+1.08	−0.61	−0.86	1.51
ref-DB-C_{60}	+1.60	–	−0.58	−1.01	–
DB-1,6-PDI-C_{60}	+0.98	+1.38	−0.58	−0.89	1.56
ref-DB-1,6-PDI	+0.93	+1.34	−0.78	−0.97	–

[a] Scan rate: 0.05 V s^{-1}. [b] Energy of charge-separated state [$E_{CS} = E_{1ox}(PDI) - E_{1red}(C_{60})$]. [c] Peaks of PDI^-, PDI^{2-}, and C_{60}^{2-} are merged.

Secondly, in the case of the single-bridged dyads, only a negligible influence of the fullerene was observed on the redox potentials of the PDI moiety, indicating almost no interaction between the two acting moieties. On the contrary, in the double-bridged dyads, a very pronounced effect of the fullerene moiety on the oxidation characteristics of the PDI moiety was observed. In the case of dyad DB-1,7-PDI-C_{60}, the first and second oxidation potentials of the PDI moiety were shifted by +180 and +210 mV, respectively. On the other hand, comparatively lower shifts of +50 and +40 mV were observed for the oxidation potentials in the dyad DB-1,6-PDI-C_{60}. This clearly indicates a more pronounced effect of the fullerene on the PDI chromophore in the dyad DB-1,7-PDI-C_{60} compared to that in DB-1,6-PDI-C_{60}.

These observations lead to the conclusion that in the double-bridged dyads the fullerene moiety influences the closely linked PDI chromophore in such a way that it does not remain as good an electron donor as it is in the ref-PDIs. Consequently, the energy of the charge-separated state is much higher in the double-bridged dyads than in the single-bridged dyads. Furthermore, since this effect of fullerene is more pronounced in the dyad DB-1,7-PDI-C_{60} than in DB-1,6-PDI-C_{60}, the difference in the energies of the charge-separated states of these two dyads is not as substantial as in the case of the single-bridged dyads. Therefore, a less pronounced difference in the photodynamics of the two double-bridged dyads, DB-1,7-PDI-C_{60} and DB-1,6-PDI-C_{60}, can be predicted.

Steady-state absorption studies: The absorption spectra of the double-bridged dyads, DB-1,7-PDI-C_{60} and DB-1,6-PDI-C_{60}, in benzonitrile are shown in Figure 4a,b, together with the spectra of the respective reference compounds.

The absorption spectra of both ref-DB-1,7-PDI and ref-DB-1,6-PDI are characterized by a broad and intense lowest-energy band corresponding to the S_0–S_1 electronic

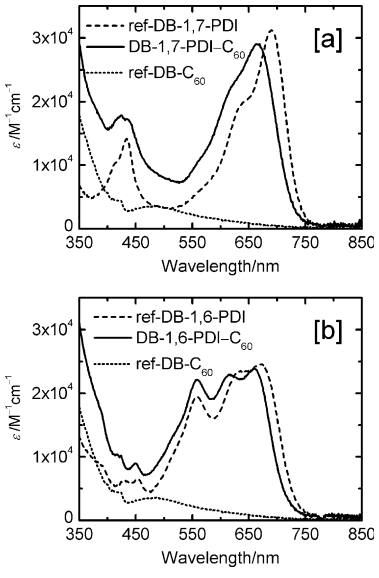

Figure 4. Steady-state absorption spectra in benzonitrile: a) DB-1,7-PDI-C_{60}, ref-DB-1,7-PDI, and ref-DB-C_{60}; b) DB-1,6-PDI-C_{60}, ref-DB-1,6-PDI, and ref-DB-C_{60}.

transition in the region 550–750 nm. However, the principal difference between these two regioisomers is evident in the region 400–500 nm. In this region, ref-DB-1,7-PDI exhibits a higher energy S_0–S_2 electronic transition centered at around 440 nm. In the case of ref-DB-1,6-PDI, the higher energy S_0–S_2 band is almost absent and the S_0–S_1 band is extended further to the green wavelengths of 500–550 nm, giving the compound its deep-blue color, whereas ref-1,7-PDI is green.

In the case of the dyads, the main absorption features of the corresponding PDI moieties are mostly preserved, and consequently the dyad DB-1,7-PDI-C_{60} is dark-green in color whereas DB-1,6-PDI-C_{60} is dark-blue. In both of the dyads, the lowest-energy band of the PDI moiety is significantly shifted to shorter wavelengths relative to those of the reference PDIs.[19] However, this blueshift is larger in DB-1,7-PDI-C_{60} than in DB-1,6-PDI-C_{60}. These results are in good agreement with those of the DPV studies, which also indicated a larger shift in the oxidation potential of the PDI moiety in DB-1,7-PDI-C_{60} than that in DB-1,6-PDI-C_{60}. As far as the single-bridged dyads are concerned, the spectra of both SB-1,7-PDI-C_{60} and SB-1,6-PDI-C_{60} correspond very closely to the sums of the spectra of the reference fullerene and the respective reference PDI (Figure S6 in the Supporting Information). These results, along with those obtained from the DPV measurements, suggest that the two acting chromophores do not mutually influence their redox or absorption properties.

Steady-state emission studies: The wavelength selected for excitation of all of the compounds was 640 nm, which provided a selective excitation of the PDI moiety (Figure S8 in the Supporting Information). In these measurements, the characteristic broad emission of the PDI moiety was found to be significantly quenched in all four of the dyads compared to the corresponding ref-PDIs. In both benzonitrile and toluene, however, more efficiently quenched emission was clearly observed for the dyads incorporating the 1,7-regioisomer of PDI compared to the corresponding dyads incorporating the 1,6-regioisomer (Table 3).

Picosecond and nanosecond transient absorption studies: In the steady-state fluorescence studies, stronger quenching of the PDI emission was observed for the dyads incorporating the 1,7-regioisomer of PDI as the donor (SB-1,7-PDI-C_{60} and DB-1,7-PDI-C_{60}) in comparison to those incorporating the 1,6-regioisomer (SB-1,6-PDI-C_{60} and DB-1,6-PDI-C_{60}). In addition, for all four of the dyads, weaker quenching was observed in nonpolar toluene than in polar benzonitrile. These variations are indicative of photoinduced electron transfer from the PDI moiety to the fullerene. Therefore, picosecond (pump–probe) and nanosecond (flash-photolysis) transient absorption methods were used to investigate the formation of the charge-separated state in these dyads and to gain a better understanding of the differences in the excited-state photodynamics between the dyads incorporating 1,7- and 1,6-substituted PDIs as donors. The excitation wavelength used to conduct these studies was 420 nm, which populates the second excited singlet state (S_2) of the PDI moiety.

Transient absorption studies of the single-bridged dyads: The decay component spectra of the single-bridged dyads, SB-1,7-PDI-C_{60} and SB-1,6-PDI-C_{60}, in benzonitrile are shown in Figure 5a, b. The components shown in the spectra were obtained by global exponential fitting of the transient absorption decay curves at different wavelengths. Consequently, the number of components should represent the number of transients in the process.

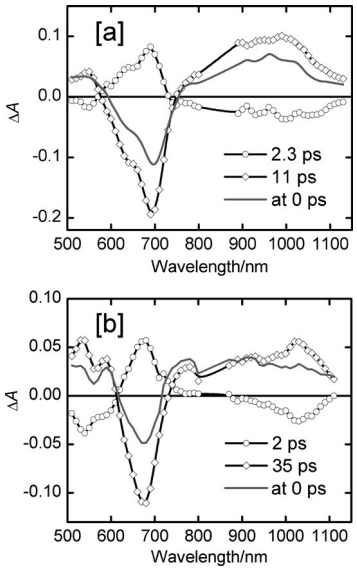

Figure 5. Picosecond transient absorption decay component spectra of a) SB-1,7-PDI-C_{60} and b) SB-1,6-PDI-C_{60} in benzonitrile.

In polar benzonitrile, only two components were obtained for both of the dyads, indicating the formation of the charge-separated (CS) state $PDI^{\bullet+}$-$C60^{\bullet-}$ from the first excited singlet state of PDI and the decay of the CS state. For both of the dyads, the longer-lived components exhibited clear indications of the existence of the charge-separated state ($PDI^{\bullet+}$-$C60^{\bullet-}$), that is, absorption at the characteristic wavelengths of the PDI radical cation at 500–600 and 720–800 nm and of the fullerene radical anion at 1000–1100 nm, which overlaps with that of the PDI radical cation at around 1000 nm.[13,20]

The shorter-lived components showed negative amplitude at the abovementioned wavelengths, and can consequently be attributed to the formation of the CS state. The CS state was formed on the same time scale (ca. 2 ps) for both of the single-bridged dyads. However, the decay of the CS state was clearly faster for the dyad SB-1,7-PDI-C_{60} (11 ps) than for the dyad SB-1,6-PDI-C_{60} (35 ps).

In nonpolar toluene, the two single-bridged dyads exhibited more pronounced differences in their photodynamics. In the pump–probe measurements, three different components were resolved for both of the dyads, as shown in Figure 6.

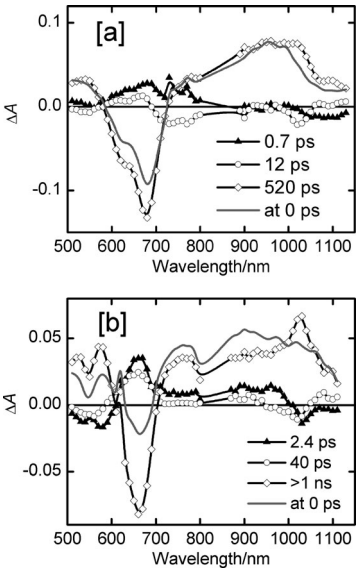

Figure 6. Picosecond transient absorption decay component spectra of a) SB-1,7-PDI-C_{60} and b) SB-1,6-PDI-C_{60} in toluene.

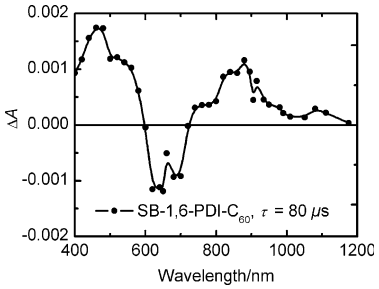

Figure 7. Nanosecond transient absorption spectrum of the dyad SB-1,6-PDI-C_{60} in toluene.

Similar shortest-lived and medium-lifetime components were also observed in the fluorescence up-conversion measurements (for further discussion, see Figure S9 in the Supporting Information and the following text). For the dyad SB-1,7-PDI-C_{60} (Figure 6a), clear evidence of the existence of the charge-separated state ($PDI^{\bullet+}$-$C60^{\bullet-}$) was provided by the longest-lived component ($\tau = 520$ ps). The medium-lifetime component ($\tau = 12$ ps) can be attributed to the formation of the charge-separated state due to negative absorption at 500–600, 720–800, and around 1020 nm, in combination with positive absorption at around 660 nm. The shortest-lived component ($\tau = 0.7$ ps) may be assigned to the formation of an intermediate exciplex state (PDI-C_{60})* preceding the charge-separated state. This intramolecular exciplex is a highly probable intermediate in these kinds of dyads, in which the donor and acceptor moieties are closely linked together.[21] This assignment is further supported by the fact that this shortest-lived component is observed only in nonpolar toluene, which favors the existence of the exciplex. For the dyad SB-1,6-PDI-C_{60} (Figure 6b), the shortest-lived ($\tau = 2.4$ ps) and medium-lifetime ($\tau = 40$ ps) components have rather similar spectral features. Considering that the exciplex is a state with a partial charge shift, that is, the electron density is delocalized over both the donor and acceptor, these components were tentatively attributed to formation of the exciplex and its decay to the charge-separated state, respectively. However, in this dyad, the decay of the charge-separated state took place on a timescale too long to be measured with the pump–probe instrument, which was limited to 1 ns.

To extract precise information about the long-lived CS state, transient absorption studies of the dyad SB-1,6-PDI-C_{60} in toluene were carried out on the nanosecond timescale by using the flash-photolysis method. The transient absorption decays were found to be mono-exponential at all of the monitoring wavelengths, and the triplet state of PDI was clearly observed as the only intermediate state (Figure 7).[17,22]

The appearance of the PDI triplet state in PDI-C_{60}-based systems in nonpolar solvents has been reported previously for dyads and dendrimer-like compounds.[17,23] Energy transfer was proposed as a possible mechanism for the formation of the PDI triplet state, in which case a cascade of processes takes place, including singlet–singlet energy transfer (from PDI to C_{60}), intersystem crossing, and triplet–triplet energy transfer (from C_{60} to PDI).[17,23] In this case, the PDI chromophore first relaxes to the ground state on a sub-nanosecond timescale and gains excitation after some delay. This is definitely not the case in the dyad SB-1,6-PDI-C_{60}, for which bleaching of the ground-state absorption (at ca. 680 nm) could be seen at any delay time. Therefore, energy transfer has no significant effect on the excitation–relaxation process in this case. Therefore, considering that the last state observed by the pump–probe method is the CS state and the only state observed by flash-photolysis is the PDI triplet state, the relaxation of the CS state to the PDI-based triplet state must take place on a timescale at some point between 1 and 50 ns, that is, within the time gap between the two instruments.

The results obtained from the picosecond and nanosecond time-resolved studies led to the conclusion that in nonpolar toluene the CS state relaxes through different pathways in the two dyads SB-1,7-PDI-C_{60} and SB-1,6-PDI-C_{60}. In SB-1,7-PDI-C_{60}, the formation of the CS state in 12 ps is followed by its decay directly to the ground state through charge recombination in 520 ps. On the other hand, in SB-1,6-PDI-C_{60}, the formation of the CS state in 40 ps is followed by its decay to the PDI triplet state on a timescale at some point in the range 1–50 ns. This PDI-based triplet state finally decays to the ground state in 80 μs. These different decay pathways pursued by the CS state in SB-1,7-PDI-C_{60} and SB-1,6-PDI-C_{60} in a nonpolar environment are summarized in Figure 8. These observations suggests that, in the dyad SB-1,7-PDI-C_{60}, the energy of the CS state is lower than that of the PDI triplet state even in a nonpolar medium. Therefore, this dyad is a promising candidate for use in solid organic photovoltaics or other optoelectronic applications.

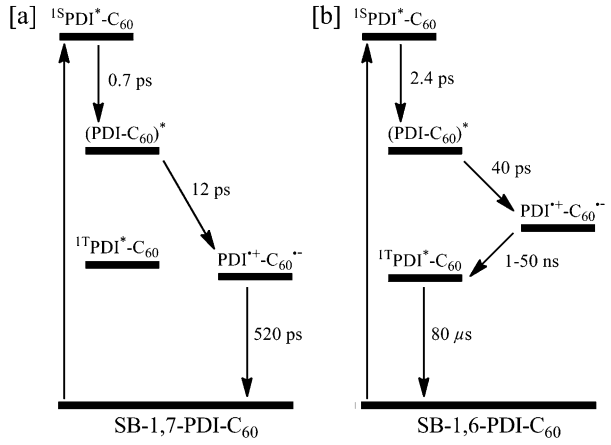

Figure 8. Photophysical pathways taking place in single-bridged dyads a) SB-1,7-PDI-C_{60} and b) SB-1,6-PDI-C_{60} in toluene.

Transient absorption studies of the double-bridged dyads: The decay component spectra of the double-bridged dyads DB-1,7-PDI-C_{60} and DB-1,6-PDI-C_{60} in benzonitrile are shown in Figure 9a,b. The two measured wavelength ranges (510–800 and 880–1130 nm) were fitted separately, and the lifetimes indicated in the figures are averages of these two results. In benzonitrile, the lifetimes obtained from the visible and NIR regions were in good agreement.

The longest-lived component gave a clear indication of the existence of the CS state (PDI$^{\bullet+}$-$C_{60}^{\bullet-}$) in both double-bridged dyads, DB-1,7-PDI-C_{60} and DB-1,6-PDI-C_{60}, that is, absorptions at the characteristic wavelengths of the PDI radical cation at 500–600 and 700–800 nm and of the bis-substituted fullerene radical anion at 900–1100 nm, the latter overlapping with the absorption of the PDI radical cation at around 1000 nm.[13,24] The medium-lifetime component shows negative amplitude at the abovementioned wavelengths and consequently corresponds to the formation of a charge-separated state. As regards the photodynamics of electron transfer, close inspection reveals differences between the two dyads. Both the formation of the CS state and its decay were found to be faster for the dyad DB-1,7-PDI-C_{60} (6 and 50 ps, respectively) than for the dyad DB-1,6-PDI-C_{60} (9 and 120 ps, respectively). For both of these double-bridged dyads, an additional component with a lifetime of less than 0.50 ps was also resolved in both benzonitrile and toluene. This shortest-lived component could be attributed to relaxation of the second excited singlet state (S_2) to the first excited singlet state of the PDI chromophore through internal conversion, since the 420 nm excitation populates the S_2 state of the PDI moiety. Similar short-lived components were also seen for the reference PDIs.

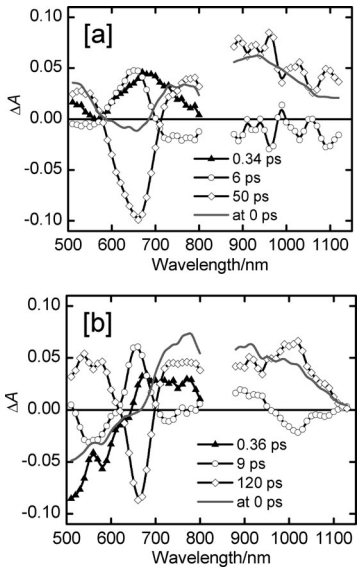

Figure 9. Picosecond transient absorption decay component spectra of a) DB-1,7-PDI-C_{60} and b) DB-1,6-PDI-C_{60} in benzonitrile.

In nonpolar toluene (Figure S11 in the Supporting Information), the medium-lifetime component again displayed some evidence of the formation of the charge-separated state, that is, negative absorptions in the regions 500–600 and 700–800 nm, coupled with a positive absorption at around 660 nm. In this case, however, the spectral changes in the NIR region were quite weak. Moreover, the lifetimes obtained from separate fittings of the visible and NIR regions were not in very good agreement. Thus, the electron transfer in the nonpolar solvent was somewhat uncertain. For both of the dyads, the decay of the tentative CS state occurs on a timescale too long to be measured with the pump–probe instrument (i.e., >1 ns). Therefore, transient absorption studies were carried out on a nanosecond timescale by using the flash-photolysis method by exciting nitrogen-purged solutions of the dyads DB-1,7-PDI-C_{60} and DB-1,6-PDI-C_{60} in toluene at 420 nm. The transient absorption spectra obtained are shown in Figures S12 and S13 in the Supporting Information.

In these measurements, for both of the dyads, the transient absorption decays were found to be mono-exponential at all monitoring wavelengths, and the triplet state of PDI was clearly observed as the only intermediate state. Thus, taking into account the time resolution of the flash-photolysis instrument, that is, approximately 50 ns, this result indicates that the relaxation of the tentative CS state to the PDI triplet state takes place on a timescale at some point between 1 and 50 ns. For both of the dyads, the PDI-based triplet state finally relaxed to the ground state on a microsecond timescale.

Furthermore, the differences in the photodynamics of the two pairs of dyads (Table 3) are also worthy of note. The energies of the CS state increase in the order SB-1,7-PDI-C_{60} < SB-1,6-PDI-C_{60} < DB-1,7-PDI-C_{60} < DB-1,6-PDI-C_{60}, and the lifetimes of the CS states in benzonitrile increase in the same order. This is consistent with a Marcus inverted regime of the electron-transfer process. However, a direct quantitative comparison with theory is complicated for these compounds due to differences in the mutual orientations of the donor and acceptor moieties in these dyads, which may affect the rate of electron transfer. Another factor affecting the rate of electron transfer is the donor–ac-

Table 3. Time constants (τ) for the ET process in all four dyads in benzonitrile and in toluene.

Compound	Solvent	Fl quenching[a]	Φ_{fl}[b]	$\tau_{exciplex}$ [ps]	τ_{CS}[c] [ps]	τ_{CR}[d]	τ_T[f] [μs]	E_{CS} [eV][g]
SB-1,7-PDI-C_{60}	PhCN	450-fold	5.3×10^{-4} (0.23)	–	2.3	11 ps	–	1.20
	toluene	130-fold	3.5×10^{-3} (0.42)	0.7	12	520 ps	–	–
SB-1,6-PDI-C_{60}	PhCN	70-fold	9.2×10^{-4} (0.07)	–	2.0	35 ps	–	1.35
	toluene	11-fold	8.6×10^{-3} (0.09)	2.4	40	1–50 ns[e]	80	–
DB-1,7-PDI-C_{60}	PhCN	390-fold	6.8×10^{-4} (0.26)	–	6	50 ps	–	1.51
	toluene	35-fold	1.2×10^{-2} (0.40)	–	400	1–50 ns[e]	65	–
DB-1,6-PDI-C_{60}	PhCN	90-fold	1.2×10^{-3} (0.10)	–	9	120 ps	–	1.56
	toluene	8-fold	1.6×10^{-2} (0.13)	–	500	1–50 ns[e]	113	–

[a] Fluorescence quenching. [b] Fluorescence quantum yields of the corresponding ref-PDIs are given in parentheses. [c] Charge separation. [d] Charge recombination. [e] Could not be determined accurately. [f] Triplet-state lifetime of PDI moiety measured by nanosecond flash-photolysis. [g] Energy of charge-separated state.

ceptor separation. According to the ^{1}H NMR, DPV, and steady-state absorption measurements discussed previously, the distance between the donor and the acceptor is shorter in the double-bridged dyads than in the single-bridged dyads. Therefore, the charge-recombination process is expected to be faster in the double-bridged dyads. Seemingly, however, this is not the case, which implies that the increase in CS state energy has a more pronounced effect than the decrease in the donor–acceptor distance. The energy increase is due in part to the decrease in electron-accepting ability (by 0.1 V; see Table 2) of bis-substituted as compared to mono-substituted fullerene, the price to be paid for using the double-linker design. The other possible explanation for the faster charge recombination in the single-bridged dyads as compared to their double-bridged counterparts is that the former have more flexibility to adopt an orientation more favorable for faster electron transfer. However, as yet we have no experimental proof of this hypothesis.

Comparing the time constants and energies of the CS states of the same regioisomers with single- or double-bridge design, it is evident that an increase in the driving force results in an increase in the reaction rate, which is consistent with the expected Marcus normal region. This dependence is broken for SB-1,7-PDI-C_{60} versus SB-1,6-PDI-C_{60}, for which electron transfer is somewhat faster in SB-1,6-PDI-C_{60} whereas the driving force is definitely higher in SB-1,7-PDI-C_{60}. Seemingly, geometric differences in the mutual arrangements of the donor and acceptor of the two dyads play an important role in this case. Another factor that may affect the observed electron-transfer rates is the possible presence of an intermediate state, an intramolecular exciplex, which was apparent in toluene, but was not spectroscopically resolved in benzonitrile.

Concluding the photochemical study, the practically important feature reported here, for the first time for PDI-C_{60} dyads, is the efficient electron transfer in both polar and nonpolar media.

Conclusion

We have developed a synthetic methodology for attachment of functionalized pyrrolidinyl groups to a PDI core to prepare mono- and bis-bay-functionalized derivatives of PDI dyes. The main importance of these derivatives lies in their potential as building blocks for the construction of complex light-harvesting arrays and artificial photosynthetic systems due to the presence of additional sites for the attachment of other chromophores close to the perylene core. Otherwise, in conventional dipyrrolidinyl-substituted PDIs (Figure 1), attachment of the chromophores is only possible at the imide positions, which causes a potential drawback of keeping the two interacting moieties significantly far from each other. The synthesis of the PDI-C_{60} dyads, as presented herein, is just one example of their utility as synthons. Upon bis-functionalization of the PDI core, we also observed differences in the chemical behavior of the 1,7- and 1,6-regioisomers. To the best of our knowledge, this is the first incidence of such a difference being discerned.

All four dyads exhibited photoinduced electron transfer in a polar medium, and the single-bridged dyads even in a nonpolar medium, which justified the strategy of attaching the fullerene at the bay region of the PDI in pursuit of more efficient photoinduced electron transfer. Specifically, the single-bridged dyad SB-1,7-PDI-C_{60} displayed highly efficient photoinduced electron transfer in a nonpolar medium, making it particularly attractive for applications in solid organic photovoltaics and optoelectronics.

This detailed comparative study of the dyads derived from the 1,7-regioisomer and the corresponding 1,6-regioisomer has exposed crucial differences in the photoinduced characteristics that may arise when two such regioisomers are deployed in a donor–acceptor-based system. The observed significant differences in the photodynamics of the single-bridged dyads are purely the result of inherently different physical properties of the 1,7- and 1,6-regioisomers. However, in the case of the double-bridged dyads, the observed differences are the net effect of different physical properties of the two regioisomers along with other dissimilarities, such as different mutual orientations of the donor–acceptor moieties and different influences of the fullerene moiety on the PDI chromophore in the two dyads. In view of these results, differences can also be anticipated in other properties of the two regioisomers. Therefore, we emphasize the need to use regioisomerically pure bay-functionalized PDIs, especially when the properties of the 1,6-regioisomer are unknown. Otherwise, contamination with the 1,6-regioisomer may significantly change the overall performance of the system. We consider these results to be highly perti-

nent in view of the widespread use of bay-functionalized PDIs in the burgeoning field of organic materials research.

Experimental Section

Materials: All reagents utilized in the syntheses were purchased from Sigma–Aldrich and were used as received unless otherwise stated. *N,N′*-Dioctyl-1,7(6)-dibromoperylene diimide (**6**) was synthesized according to the procedure described in the literature.[11,12a] L-*N*-Boc-Proline (**2**), L-2-(hydroxymethyl)-*N*-Boc-pyrrolidine (**3**), and the reference fullerenes (ref-DB-C_{60} and ref-SB-C_{60}) were synthesized according to literature protocols.[25]

Instrumentation and characterization: NMR spectra were recorded on a Varian Mercury 300 MHz spectrometer from solutions in $CDCl_3$ at room temperature. All chemical shifts are quoted relative to TMS (δ = 0.0 ppm); δ values are given in ppm and J values in Hz. High-resolution mass spectra were measured on a Waters LCT Premier XE ESI-TOF benchtop mass spectrometer. To obtain accurate mass values, we simultaneously infused the solution of the reference compound (leucine enkephaline) with analyte, and processed the experimental spectra according to the routine of accurate mass measurements (peak centering and lock-mass TOF correction). Differential pulse voltammetry was performed by using a potentiostat (Iviumstat compactstat IEC 61326 Standard) controlled by a PC with the software Iviumsoft (version 1.752). The solution was placed in a three-electrode single-compartment cell consisting of platinum in glass as the working electrode, Ag/AgCl as the reference electrode, and a graphite rod as the counter electrode. During the measurements, the values of pulse height, pulse width, and step voltage were set at 20 mV, 20 ms, and 2.5 mV, respectively. A 0.1 M solution of tetrabutylammonium tetrafluoroborate in benzonitrile was used as the supporting electrolyte. Measurements were made under a continuous flow of nitrogen. An Fc/Fc^+ couple was used as an internal standard, which exhibited oxidation at +0.48 V. The measurements were carried out in both directions: toward positive and negative potentials. The reduction and oxidation potentials were calculated as an average of the two scans.

All of the spectroscopic measurements were carried out at room temperature. Absorption spectra were recorded on a Shimadzu UV-2501PC spectrophotometer and fluorescence spectra on a Fluorolog-3 (SPEX Inc.) fluorimeter. The emission spectra were corrected by using a correction function supplied by the manufacturer. Fluorescence quantum yields were determined relative to cresyl violet (Φ_f = 0.54 in methanol).[26] The specified quantum yields are averages of values measured at three different excitation wavelengths. Optical densities at excitation wavelengths were maintained at around 0.1 to avoid re-absorption.

The flash-photolysis method was used to study time-resolved absorption on the nano- to microsecond timescale with 10 ns laser pulses. The instrument has been described in detail elsewhere.[27] The samples were deoxygenated by bubbling nitrogen through the solutions, which was started 30 min prior to the first measurement and continued throughout. The optical density of solutions at the excitation wavelength was maintained at around 0.6, and the excitation power density was 1 mJ cm^{-2}. The pump–probe technique was used to detect fast processes taking place on the picosecond timescale. The instrument and the data analysis procedure used have been described previously.[21b,28]

Synthesis of 2-(benzyloxymethyl)-*N*-Boc-pyrrolidine (4): A solution of 2-(hydroxymethyl)-*N*-Boc-pyrrolidine (**3**; 2.40 g, 11.92 mmol) in dry THF (20 mL) was added to a mechanically stirred suspension of sodium hydride (60%; 0.60 g, 15.00 mmol) in dry THF (20 mL). The reaction mixture was stirred for 1 h at room temperature. Thereafter, benzyl bromide (2.43 mL, 20.43 mmol) was added dropwise and the mixture was stirred for a further 20 h at room temperature. The reaction mixture was then poured into brine (20 mL) and extracted with ethyl acetate (4×50 mL). The combined organic phases were dried over sodium sulfate and concentrated in vacuo. The resultant crude oily residue was purified on silica-60, eluting first with hexane to remove the benzyl bromide and then with hexane/ethyl acetate (10:1) to collect the product as a yellow oil (2.82 g, 80.4%). ^{1}H NMR (300 MHz, $CDCl_3$, TMS): δ = 7.42–7.21 (m, 5H), 4.52 (s, 2H), 4.11–3.81 (m, 1H), 3.71–3.51 (m, 1H), 3.49–3.16 (m, 3H), 2.07–1.68 (m, 4H), 1.43 ppm (s, 9H); MS (ESI-TOF): calcd for $C_{17}H_{25}NO_3$: 292.1913 $[M+H]^+$; found: 292.1912.

Synthesis of 2-(benzyloxymethyl)pyrrolidine (5): 2-(Benzyloxymethyl)-*N*-Boc-pyrrolidine (**4**; 1.35 g, 4.64 mmol) was dissolved in dichloromethane (6.20 mL), TFA (1.20 mL) was then added, and the reaction mixture was stirred for 3 h at room temperature. The progress of the reaction was followed by TLC analysis of removed aliquots ($CHCl_3$/EtOH, 18:1). After complete consumption of the starting material, the TFA and CH_2Cl_2 were evaporated under reduced pressure. The crude oily residue was dissolved in ethyl acetate (30 mL) and the solution was washed with saturated aqueous $NaHCO_3$. The organic phase was dried over sodium sulfate and concentrated. The crude product was then purified by column chromatography on silica-100 ($CHCl_3$ and $CHCl_3$/EtOH, 5:1) to afford the product as a yellow viscous oil (0.56 g, 63.0%). ^{1}H NMR (300 MHz, $CDCl_3$, TMS): δ = 7.40–7.15 (m, 5H), 6.72 (s, 1H), 4.48 (s, 2H), 3.60–3.20 (m, 3H), 3.15–2.78 (m, 2H), 1.95–1.42 ppm (m, 4H); MS (ESI-TOF): calcd for $C_{12}H_{17}NO$: 192.1388 $[M+H]^+$; found: 192.1395.

The optical purities of compounds **4** and **5** and their possible racemization during the course of the performed reactions were not determined.

Synthesis of *N,N′*-dioctyl-1-bromo-7(6)-[2-(benzyloxymethyl)pyrrolidinyl]perylene-3,4,9,10-tetracarboxy diimide (7): A 3:1 regioisomeric mixture of *N,N′*-dioctyl-1,7- and -1,6-dibromoperylene diimides **6** (110 mg, 0.14 mmol) was suspended in dry toluene (4 mL) in a closed vial. 2-(Benzyloxymethyl)pyrrolidine (**5**; 400 mg, 2.08 mmol) was then added. The reaction mixture was purged with argon for 10 min and then stirred for 19 h at 100 °C. After being cooled to room temperature, the reaction mixture was poured into water (100 mL) and the resulting mixture was extracted with CH_2Cl_2 (2×75 mL). The combined organic layers were dried over anhydrous sodium sulfate and concentrated under reduced pressure. The resultant green residue was subjected to column chromatography (silica-60; CH_2Cl_2) to afford the desired product **7** (95.1 mg, 75.7%) as a green solid. Around 20 mg (18.2%) of unreacted starting material **6** was recovered. ^{1}H NMR (300 MHz, $CDCl_3$, TMS): δ = 9.45 (d, J = 8.2 Hz, 1.1H), 8.85 (s, 0.8H), 8.74 (s, 0.2H), 8.69 (s, 0.3H), 8.67 (0.8H), 8.47 (d, J = 8.2 Hz, 1H), 8.38 (d, J = 7.9 Hz, 0.8H), 7.83 (d, J = 8.2 Hz, 0.2H), 7.76 (d, J = 7.9 Hz, 0.7H), 7.39–7.30 (m, 5H), 4.78–4.66 (m, 1H), 4.61 (s, 1.8H), 4.51 (s, 0.2H), 4.26–4.14 (m, 4H), 4.10–4.02 (m, 1H), 3.82–3.74 (m, 1H), 3.70–3.36 (m, 2H), 2.37–1.84 (m, 4H), 1.83–1.68 (m, 4H), 1.35–1.15 (m, 20H), 0.88 ppm (m, 6H); MS (ESI-TOF): calcd for $C_{52}H_{56}BrN_3O_5$: 881.3403 $[M]^+$; found: 881.3433.

Synthesis of *N,N′*-dioctyl-1-[2-(benzyloxymethyl)pyrrolidinyl]perylene-3,4,9,10-tetracarboxy diimide (8) and *N,N′*-dioctyl-1,7(6)-bis[2-(benzyloxymethyl)pyrrolidinyl]perylene-3,4,9,10-tetracarboxy diimide (9): A 3:1 regioisomeric mixture of *N,N′*-dioctyl-1,7- and -1,6-dibromoperylene diimides **6** (100 mg, 0.13 mmol) was suspended in dry toluene (5 mL) in a closed vial. 2-(Benzyloxymethyl)pyrrolidine (**5**; 2.20 g, 11.51 mmol) was then added. The reaction mixture was purged with argon for 10 min and then stirred for 18 h at 100 °C. After being cooled to room temperature, the reaction mixture was poured into water (30 mL) and extracted with CH_2Cl_2 (2×50 mL). The combined organic phases were dried over anhydrous sodium sulfate and then concentrated by rotary evaporation. The resultant green residue was purified by column chromatography (silica-60; CH_2Cl_2) to afford a mixture of *N,N′*-dioctyl-1-[2-(benzyloxymethyl)-pyrrolidinyl]perylene diimide **8** and the desired product *N,N′*-dioctyl-1,7(6)-bis[2-(benzyloxymethyl)pyrrolidinyl]perylene diimide **9**. This mixture was finally separated on HPTLC glass plates ($CHCl_3$/toluene, 2:1) to yield **8** (73.5 mg, 70.5%) as a dark-green solid and **9** (25.5 mg, 19.8%) as a bluish-green solid. The desired product **9** was a mixture of 1,7- and 1,6-regioisomers in a 1:1 ratio, as revealed by ^{1}H NMR analysis. The two regioisomers could not be separated and were therefore used as a mixture for the next reaction.

*N,N′-Dioctyl-1-[2-(benzyloxymethyl)pyrrolidinyl]perylene diimide (**8**)*: ^{1}H NMR (300 MHz, $CDCl_3$, TMS): δ = 8.65 (s, 1H), 8.54 (d, J = 8.2 Hz, 1H), 8.47–8.28 (m, 4H), 7.90 (d, J = 8.2 Hz, 1H), 7.44–7.39 (m, 5H), 4.73–4.60 (m, 3H), 4.26–4.14 (m, 4H), 4.09–3.99 (m, 1H), 3.86–3.75 (m, 1H), 3.67–3.44 (m, 1H), 2.38–2.12 (m, 2H), 2.10–1.92 (m, 2H), 1.91–1.67

(m, 5H), 1.44–1.23 (m, 20H), 0.87 ppm (m, 6H); MS (ESI-TOF): calcd for $C_{52}H_{57}N_3O_5$: 803.4298 $[M]^+$; found: 803.4354.

N,N′-*Dioctyl-1,7(6)-bis[2-(benzyloxymethyl)pyrrolidinyl]perylene diimide* (***9***): ^{1}H NMR (300 MHz, $CDCl_3$, TMS): δ = 8.63 (s, 1H), 8.52–8.46 (m, 2H), 8.25 (d, J = 7.9 Hz, 1H), 8.19 (d, J = 7.9 Hz, 1H), 8.07 (d, J = 8.2 Hz, 1H), 7.40–7.28 (m, 10H), 4.69–4.56 (m, 6H), 4.28–4.16 (m, 5H), 4.04–3.89 (m, 3H), 3.86–3.76 (m, 2H), 3.66–3.46 (m, 3H), 2.34–2.10 (m, 6H), 1.82–1.70 (m, 5H), 1.41–1.22 (m, 20H), 0.93–0.84 ppm (m, 6H); MS (ESI-TOF): calcd for $C_{64}H_{72}N_4O_6$: 992.5452 $[M]^+$; found: 992.5453.

Synthesis of *N,N′*-dioctyl-1,7- and -1,6-bis[2-(hydroxymethyl)pyrrolidinyl]perylene-3,4,9,10-tetracarboxy diimides (10 and 11): A 1:1 regioisomeric mixture of *N,N′*-dioctyl-1,7- and -1,6-bis[2-(benzyloxymethyl)pyrrolidinyl]perylene diimides **9** (100 mg, 0.10 mmol) was dissolved in dry CH_2Cl_2 (10 mL) and the solution was cooled to −78 °C. BBr_3 (1 M solution in CH_2Cl_2, 210 μL, 0.21 mmol) was then added, and the reaction mixture was stirred at −78 °C for 45 min. The progress of the reaction was monitored by TLC analysis of removed aliquots ($CHCl_3$/EtOH, 50:1). When the starting material had been essentially consumed, the reaction was quenched by the addition of MeOH (20 mL). Further CH_2Cl_2 (10 mL) was added and the solution was washed with water (3×30 mL). The organic phase was collected, dried over sodium sulfate, and concentrated. The crude residue was first purified by column chromatography on silica-100 ($CHCl_3$ and $CHCl_3$/EtOH, 50:1) to obtain a regioisomeric mixture of **10** and **11** (52.7 mg, 64.4%). The regioisomers were finally separated on HPTLC glass plates to yield *N,N′*-dioctyl-1,7-bis[2-(hydroxymethyl)pyrrolidinyl]perylene diimide **10** (12.8 mg, 15.6%) as a dark-green solid and *N,N′*-dioctyl-1,6-bis[2-(hydroxymethyl)pyrrolidinyl]-perylene diimide **11** (15.5 mg, 18.9%) as a dark-blue solid.

N,N′-*Dioctyl-1,7-bis[2-(hydroxymethyl)pyrrolidinyl]perylene diimide* (***10***): ^{1}H NMR (300 MHz, $CDCl_3$, TMS): δ = 8.46 (s, 2H), 8.35 (d, J = 8.1 Hz, 2H), 7.92 (d, J = 8.1 Hz, 2H), 4.45 (br s, 2H), 4.26–4.11 (m, 7H), 4.07–3.95 (m, 3H), 3.88–3.76 (m, 1H), 3.64–3.47 (m, 2H), 2.95–2.75 (m, 1H), 2.40–2.18 (m, 4H), 2.07–1.88 (m, 4H), 1.80–1.68 (m, 4H), 1.46–1.19 (m, 20H), 0.93–0.79 ppm (m, 6H); MS (ESI-TOF): calcd for $C_{50}H_{60}N_4O_6$: 812.4513 $[M]^+$; found: 812.4530.

N,N′-*Dioctyl-1,6-bis[2-(hydroxymethyl)pyrrolidinyl]perylene diimide* (***11***): ^{1}H NMR (300 MHz, $CDCl_3$, TMS): δ = 8.68 (d, J = 8.0 Hz, 2H), 8.47 (s, 2H), 8.24 (d, J = 8.0 Hz, 2H), 4.52 (br s, 2H), 4.29–3.93 (m, 8H), 3.87–3.50 (m, 4H), 2.90–2.70 (m, 1H), 2.40–1.89 (m, 8H), 1.80–1.69 (m, 6H), 1.43–1.20 (m, 20H), 0.94–0.80 ppm (m, 6H); MS (ESI-TOF): calcd for $C_{50}H_{60}N_4O_6$: 812.4513 $[M]^+$; found: 812.4550.

Synthesis of *N,N′*-dioctyl-1,7-bis[2-(ethoxymalonateoxymethyl)pyrrolidinyl]perylene-3,4,9,10-tetracarboxy diimide (12): In a typical reaction, *N,N′*-dioctyl-1,7-bis[2-(hydroxymethyl)pyrrolidinyl]perylene diimide **10** (12.8 mg, 15.8 μmol) was dissolved in CH_2Cl_2 (12 mL) and the solution was cooled in an ice bath. Et_3N (6.6 μL, 47.4 μmol) and ethyl malonyl chloride (6.1 μL, 47.4 μmol) were then added and the reaction mixture was stirred for 3 h at room temperature. Thereafter, the solvent was removed by rotary evaporation and the solid residue was chromatographed on silica-60, eluting with $CHCl_3$, to afford **12** (13.8 mg, 84.1%) as a green solid. ^{1}H NMR (300 MHz, $CDCl_3$, TMS): δ = 8.66 (s, 2H), 8.49 (d, J = 8.1 Hz, 2H), 8.14 (d, J = 8.1 Hz, 2H), 4.75–4.51 (m, 4H), 4.26–4.14 (m, 8H), 3.76–3.58 (m, 3H), 3.48 (s, 4H), 2.44–2.12 (m, 3H), 2.08–1.92 (m, 4H), 1.84–1.67 (m, 6H), 1.43–1.20 (m, 28H), 0.93–0.78 ppm (m, 6H); MS (ESI-TOF): calcd for $C_{60}H_{72}N_4O_{12}$: 1040.5146 $[M]^+$; found: 1040.5170.

Synthesis of DB-1,7-PDI-C_{60} (13): I_2 (3.5 mg, 13.8 μmol) and *N,N′*-dioctyl-1,7-bis[2-(ethoxymalonateoxymethyl)pyrrolidinyl]perylene diimide **12** (7.1 mg, 6.8 μmol) were added to a clear solution of C_{60} (5.3 mg, 7.4 μmol) in toluene (100 mL). The resulting solution was stirred for 15 min at room temperature under argon atmosphere. DBU (5.7 μL, 40.4 μmol) was then added, and the reaction mixture was stirred for a further 40 min at room temperature under argon atmosphere. Thereafter, the toluene was removed by rotary evaporation. The solid green residue was first purified by column chromatography (silica-60; $CHCl_3$) and subsequently on HPTLC glass plates eluting with $CHCl_3$ to afford the desired dyad **13** as a green solid (4.5 mg, 37.6%). ^{1}H NMR (300 MHz, $CDCl_3$, TMS): δ = 9.67 (d, J = 8.2 Hz, 1H), 9.02 (s, 1H), 8.59 (d, J = 8.0 Hz, 1H), 8.38 (s, 1H), 8.41–8.27 (m, 2H), 5.34–5.16 (m, 1H), 4.85 (d, J = 11.3 Hz, 2H), 4.70–4.40 (m, 5H), 4.39–4.10 (m, 8H), 4.05–3.30 (m, 4H), 2.60–1.90 (m, 10H), 1.87–1.64 (m, 6H), 1.40–1.20 (m, 20H), 0.94–0.80 ppm (m, 6H); MS (ESI-TOF): calcd for $C_{120}H_{68}N_4O_{12}$: 1757.4867 $[M]^+$; found: 1757.4926.

Synthesis of *N,N′*-dioctyl-1,6-bis[2-(ethoxymalonateoxymethyl)pyrrolidinyl]perylene-3,4,9,10-tetracarboxy diimide (14): The title compound was prepared from *N,N′*-dioctyl-1,6-bis[2-(hydroxymethyl)pyrrolidinyl]perylene diimide **11** (10.6 mg, 13.1 μmol), Et_3N (3.8 μL, 27.3 μmol), and ethyl malonyl chloride (5.0 μL, 39.0 μmol) following the procedure described above for compound **12**. The crude product was purified by column chromatography (silica-60; $CHCl_3$) to afford the purified compound **14** (12.1 mg, 89%) as a deep-blue solid. ^{1}H NMR (300 MHz, $CDCl_3$, TMS): δ = 8.69 (d, J = 8.1 Hz, 2H), 8.51 (s, 2H), 8.29 (d, J = 8.1 Hz, 2H), 4.70–4.46 (m, 5H), 4.27–4.13 (m, 8H), 4.10–3.90 (m, 2H), 3.80–3.55 (m, 2H), 3.45 (s, 4H), 2.41–2.26 (m, 2H), 2.09–1.91 (br m, 6H), 1.84–1.67 (m, 6H), 1.43–1.21 (m, 25H), 0.95–0.84 ppm (m, 6H); MS (ESI-TOF): calcd for $C_{60}H_{72}N_4O_{12}Na$: 1063.5044 $[M+Na]^+$; found: 1063.5046.

Synthesis of DB-1,6-PDI-C_{60} (15): I_2 (5.9 mg, 23.2 μmol) and *N,N′*-dioctyl-1,6-bis[2-(ethoxymalonateoxymethyl)pyrrolidinyl]perylene diimide **14** (12.1 mg, 11.6 μmol) were added to a clear solution of C_{60} (9.2 mg, 12.8 μmol) in toluene (170 mL). The resulting solution was stirred for 15 min under argon atmosphere. DBU (9.8 μL, 69.6 μmol) was then added, and the reaction mixture was stirred for a further 40 min at room temperature under argon atmosphere. Thereafter, the toluene was removed by rotary evaporation. The solid residue was first purified by column chromatography (silica-60; $CHCl_3$) and subsequently on HPTLC glass plates to afford the desired dyad **15** as a blue solid (6.2 mg, 30.4%). ^{1}H NMR (300 MHz, $CDCl_3$, TMS): δ = 9.14 (s, 1H), 8.67 (d, J = 8.1 Hz, 1H), 8.48 (d, J = 8.0 Hz, 1H), 8.43 (s, 1H), 7.39 (d, J = 8.0 Hz, 1H), 7.32 (d, J = 8.1 Hz, 1H), 5.08 (d, J = 11.1 Hz, 1H), 5.03–4.89 (m, 2H), 4.80–4.67 (m, 1H), 4.64–4.48 (m, 2H), 4.32 (d, J = 10.8 Hz, 1H), 4.27–4.11 (m, 5H), 4.02–3.36 (m, 6H), 2.60–1.70 (m, 11H), 1.42–1.08 (m, 26H), 0.94–0.72 ppm (m, 7H); MS (ESI-TOF): calcd for $C_{120}H_{68}N_4O_{12}$: 1757.4867 $[M]^+$; found: 1757.4940.

Synthesis of *N,N′*-dioctyl-1-pyrrolidinyl-7(6)-[2-(benzyloxymethyl)pyrrolidinyl]perylene-3,4,9,10-tetracarboxy diimide (16): *N,N′*-Dioctyl-1-bromo-7(6)-[2-(benzyloxymethyl)pyrrolidinyl]perylene diimide **7** (65 mg, 0.07 mmol) was dissolved in pyrrolidine (10 mL) and the solution was stirred for 8 h at 60 °C in a closed vial. The progress of the reaction was followed by TLC analysis of removed aliquots. When the starting material had been essentially consumed, the reaction was quenched by the addition of water (30 mL). The product was extracted with CH_2Cl_2 (50 mL) and the organic phase was washed with several portions of water to completely remove the pyrrolidine. The organic phase was collected, dried over sodium sulfate, and concentrated. The crude residue was purified by column chromatography (silica-60; CH_2Cl_2) to afford the desired product **16** (45.1 mg, 64%) as a regioisomeric mixture. ^{1}H NMR (300 MHz, $CDCl_3$, TMS): δ = 8.65 (d, J = 8.2 Hz, 0.14H), 8.55 (s, 0.63H), 8.51–8.46 (br m, 0.21H), 8.41 (br s, 0.21H), 8.38–8.31 (m, 1H), 8.30–8.15 (m, 2H), 8.00 (d, J = 8.2 Hz, 0.83H), 7.81 (d, J = 8.4 Hz, 0.1H), 7.48 (d, J = 7.9 Hz, 0.77H), 7.43–7.29 (m, 4H), 6.90–6.30 (m, 1H), 4.82–4.51 (m, 2H), 4.32–4.15 (m, 4H), 4.10–3.45 (m, 6H), 2.40–1.90 (m, 7H), 1.86–1.71 (m, 5H), 1.53–1.18 (m, 20H), 0.93–0.82 ppm (m, 6H); MS (ESI-TOF): calcd for $C_{56}H_{64}N_4O_5$: 872.4877 $[M]^+$; found: 872.4965.

Synthesis of *N,N′*-dioctyl-1-pyrrolidinyl-7-[2-(hydroxymethyl)pyrrolidinyl]perylene-3,4,9,10-tetracarboxy diimide (17) and *N,N′*-dioctyl-1-pyrrolidinyl-6-[2-(hydroxymethyl)pyrrolidinyl]perylene-3,4,9,10-tetracarboxy diimide (18): *N,N′*-Dioctyl-1-pyrrolidinyl-7(6)-[2-(benzyloxymethyl)pyrrolidinyl]perylene diimide **16** (270.0 mg, 0.31 mmol) was dissolved in dry CH_2Cl_2 (100 mL). The solution was cooled in an ice bath for 30 min under an inert atmosphere. BBr_3 (1 M solution in CH_2Cl_2, 1.1 mL, 1.1 mmol) was then added in three portions at intervals of 20 min. The progress of the reaction was closely monitored by TLC analysis of removed aliquots. After complete consumption of the starting material, the reaction was quenched by the addition of MeOH (50 mL). The organic phase was washed with water (2×100 mL), dried over sodium sulfate, and concentrated. The green solid residue was purified by column chromatography (silica-60; $CHCl_3$) to afford a mixture of the desired products

17 and **18** (240.0 mg, 99.1 %). In order to separate the regioisomers, the mixture was further chromatographed on silica-60 (75 mL; CH_2Cl_2/$CHCl_3$, 1:1). The first portion (120 mL) of the main fraction was blue in color and was collected separately. The rest of the main fraction was collected and concentrated to yield **17** (184.2 mg, 76.1 %) as a dark-green solid. The blue fraction was purified twice more to obtain **18** (17.7 mg, 7.3 %) as a dark-blue solid.

*N,N′-Dioctyl-1-pyrrolidinyl-7-[2-(hydroxymethyl)pyrrolidinyl]perylene diimide (**17**)*: ^{1}H NMR (300 MHz, $CDCl_3$, TMS): δ = 8.45 (s, 1H), 8.30 (d, J = 7.9 Hz, 1H), 8.25 (d, J = 7.9 Hz, 1H), 7.98 (s, 1H), 7.72 (d, J = 7.9 Hz, 1H), 7.36 (d, J = 7.9 Hz, 1H), 4.47–4.33 (m, 1H), 4.33–4.10 (m, 5H), 3.95 (br d, 1H), 3.76 (br s, 1H), 3.59–3.33 (m, 3H), 3.06–2.92 (m, 1H), 2.30–1.65 (m, 12H), 1.45–1.20 (m, 22H), 0.93–0.81 ppm (m, 6H); MS (ESI-TOF): calcd for $C_{49}H_{58}N_4O_5$: 782.4407 $[M]^+$; found: 782.4364.

*N,N′-Dioctyl-1-pyrrolidinyl-6-[2-(hydroxymethyl)pyrrolidinyl]perylene diimide (**18**)*: ^{1}H NMR (300 MHz, $CDCl_3$, TMS): δ = 8.59 (d, J = 7.9 Hz, 1H), 8.45 (s, 1H), 8.40 (d, J = 7.9 Hz, 1H), 8.33–8.22 (m, 2H), 7.41 (d, J = 8.2 Hz, 1H), 4.48 (br s, 1H), 4.25–3.92 (m, 6H), 3.80–3.52 (m, 3H), 3.21 (br s, 1H), 2.38–2.20 (m, 2H), 2.14–1.90 (m, 6H), 1.82–1.55 (m, 7H), 1.50–1.20 (m, 20H), 0.94–0.82 ppm (m, 6H); MS (ESI-TOF): calcd for $C_{49}H_{58}N_4O_5$: 782.4407 $[M]^+$; found: 782.4401.

Synthesis of *N,N′*-dioctyl-1-pyrrolidinyl-7-[2-(ethoxymalonateoxymethyl)-pyrrolidinyl]perylene-3,4,9,10-tetracarboxy diimide (19): *N,N′*-Dioctyl-1-pyrrolidinyl-7-[2-(hydroxymethyl)pyrrolidinyl]perylene diimide **17** (24.0 mg, 30.6 μmol) was dissolved in CH_2Cl_2 (10 mL) and the solution was cooled in an ice bath for 30 min. Et_3N (5.2 μL, 37.2 μmol) and ethyl malonyl chloride (8.0 μL, 62.2 μmol) were then added, and the reaction mixture was stirred for 1 h at room temperature. The solvent was removed by rotary evaporation and the solid residue was chromatographed on silica-100 eluting with $CHCl_3$ to afford **19** (26.1 mg, 95 %) as a deep-green solid. ^{1}H NMR (300 MHz, $CDCl_3$, TMS): δ = 8.64 (s, 1H), 8.48 (s, 1H), 8.46 (d, J = 8.2 Hz, 2H), 8.20 (d, J = 8.2 Hz, 1H), 7.64 (d, J = 8.2 Hz, 1H), 4.73–4.45 (m, 2H), 4.28–4.10 (m, 6H), 4.08–3.60 (m, 4H), 3.49 (s, 2H), 2.40–1.90 (m, 6H), 1.83–1.63 (m, 5H), 1.43–1.15 (m, 27H), 0.91–0.79 ppm (m, 6H); MS (ESI-TOF): calcd for $C_{54}H_{64}N_4O_8Na$: 919.4622 $[M+Na]^+$; found: 919.4663.

Synthesis of SB-1,7-PDI-C_{60} (20): I_2 (3.6 mg, 14.1 μmol) and *N,N′*-dioctyl-1-pyrrolidinyl-7-[2-(ethoxymalonateoxymethyl)pyrrolidinyl]perylene diimide **19** (12.7 mg, 14.1 μmol) were added to a clear solution of C_{60} (11.2 mg, 15.5 μmol) in toluene (150 mL). The resulting solution was stirred for 15 min at room temperature under argon atmosphere. DBU (6.0 μL, 44.7 μmol) was then added, and the reaction mixture was stirred for a further 45 min at room temperature. The toluene was evaporated under reduced pressure. The solid green residue was first purified by column chromatography (silica-60; $CHCl_3$) and subsequently on HPTLC glass plates eluting with $CHCl_3$ to afford SB-1,7-PDI-C_{60} **20** (11.3 mg, 49.4 %) as a dark-green solid. ^{1}H NMR (300 MHz, $CDCl_3$, TMS): δ = 9.02 (s, 1H), 8.50–8.38 (m, 2H), 8.37–8.27 (m, 2H), 7.51 (d, J = 8.1 Hz, 1H), 5.17–5.03 (m, 1H), 4.90–4.60 (m, 3H), 4.28–4.06 (m, 4H), 4.04–3.50 (m, 5H), 2.27–1.85 (m, 6H), 1.63–1.49 (m, 7H), 1.44–1.20 (m, 24H), 0.93–0.79 ppm (m, 6H); MS (ESI-TOF): calcd for $C_{114}H_{62}N_4O_8Cl$: 1650.4290 $[M+Cl]^-$; found: 1650.4324.

Synthesis of *N,N′*-dioctyl-1-pyrrolidinyl-6-[2-(ethoxymalonateoxymethyl)-pyrrolidinyl]perylene-3,4,9,10-tetracarboxy diimide (21): This compound was prepared from *N,N′*-dioctyl-1-pyrrolidinyl-6-[2-(hydroxymethyl)pyrrolidinyl]perylene diimide **18** (10.0 mg, 12.8 μmol) following the procedure described above for compound **19** to afford the purified compound **21** (11.0 mg, 96.0 %) as a deep-blue solid. ^{1}H NMR (300 MHz, $CDCl_3$, TMS): δ = 8.74–8.62 (m, 2H), 8.54–8.42 (m, 2H), 8.38 (s, 1H), 7.71 (d, J = 7.9 Hz, 1H), 4.70–4.40 (m, 3H), 4.33–4.12 (m, 6H), 3.90–3.54 (m, 4H), 3.43 (s, 2H), 2.43–2.25 (m, 1H), 2.19–1.86 (m, 6H), 1.86–1.65 (m, 6H), 1.56–1.17 (m, 24H), 0.95–0.80 ppm (m, 6H); MS (ESI-TOF): calcd for $C_{54}H_{64}N_4O_8Na$: 919.4622 $[M+Na]^+$; found: 919.4620.

Synthesis of SB-1,6-PDI-C_{60} (22): This compound was prepared from *N,N′*-dioctyl-1-pyrrolidinyl-6-[2-(ethoxymalonateoxymethyl)pyrrolidinyl]-perylene diimide **21** (12.0 mg, 13.4 μmol) following the procedure described above for compound **20** to afford SB-1,6-PDI-C_{60} (**22**; 9.0 mg, 40.7 %) as a deep-blue solid. ^{1}H NMR (300 MHz, $CDCl_3$, TMS): δ = 8.85 (s, 1H), 8.68 (d, J = 7.9 Hz, 1H), 8.63 (d, J = 7.9 Hz, 1H), 8.39 (d, J = 8.2 Hz, 1H), 8.20 (s, 1H), 7.41 (d, J = 7.9 Hz, 1H), 5.12–4.98 (m, 1H), 4.91–4.60 (m, 4H), 4.27–4.05 (m, 4H), 3.80–3.60 (m, 2H), 3.58–3.42 (m, 2H), 2.54–2.39 (m, 1H), 2.20–1.89 (m, 6H), 1.83–1.68 (m, 4H), 1.66–1.55 (m, 6H), 1.50–1.19 (m, 22H), 0.94–0.82 ppm (m, 6H); MS (ESI-TOF): calcd for $C_{114}H_{62}N_4O_8Na$: 1638.4498 $[M+Na]^+$; found: 1638.4448.

Acknowledgements

The authors are grateful to the Academy of Finland for financial support.

[1] a) C. Huang, S. Barlow, S. R. Marder, *J. Org. Chem.* **2011**, *76*, 2386–2407; b) F. Würthner, *Chem. Commun.* **2004**, 1564–1579.
[2] a) R. Schmidt, M. M. Ling, J. H. Oh, M. Winkler, M. Könemann, Z. Bao, F. Würthner, *Adv. Mater.* **2007**, *19*, 3692–3695; b) Z. Chen, M. G. Debije, T. Debaerdemaeker, P. Osswald, F. Würthner, *ChemPhysChem* **2004**, *5*, 137–140; c) M. J. Ahrens, M. J. Fuller, M. R. Wasielewski, *Chem. Mater.* **2003**, *15*, 2684–2686; d) Y. Zhao, M. R. Wasielewski, *Tetrahedron Lett.* **1999**, *40*, 7047–7050; e) C. Kohl, T. Weil, J. Qu, K. Müllen, *Chem. Eur. J.* **2004**, *10*, 5297–5310; f) G. Balaji, T. S. Kale, A. Keerthi, A. M. D. Pelle, S. Thayumanavan, S. Valiyaveettil, *Org. Lett.* **2011**, *13*, 18–21.
[3] B. A. Jones, M. J. Ahrens, M. H. Yoon, A. Facchetti, T. J. Marks, M. R. Wasielewski, *Angew. Chem.* **2004**, *116*, 6523–6526; *Angew. Chem. Int. Ed.* **2004**, *43*, 6363–6366.
[4] a) P. Ranke, I. Bleyl, J. Simmerer, D. Haarer, A. Bacher, H. W. Schmidt, *Appl. Phys. Lett.* **1997**, *71*, 1332–1334; b) M. A. Angadi, D. Gosztola, M. R. Wasielewski, *Mater. Sci. Eng. B* **1999**, *63*, 191–194.
[5] X. Guo, D. Zhang, D. Zhu, *Adv. Mater.* **2004**, *16*, 125–130.
[6] C. Li, H. Wonneberger, *Adv. Mater.* **2012**, *24*, 613–636.
[7] J. Baffreau, S. Leroy-Lhez, N. V. Anh, R. M. Williams, P. Hudhomme, *Chem. Eur. J.* **2008**, *14*, 4974–4992.
[8] X. He, H. Liu, Y. Li, S. Wang, Y. Li, N. Wang, J. Xiao, X. Xu, D. Zhu, *Adv. Mater.* **2005**, *17*, 2811–2815.
[9] E. A. Weiss, M. J. Ahrens, L. E. Sinks, A. V. Gusev, M. A. Ratner, M. R. Wasielewski, *J. Am. Chem. Soc.* **2004**, *126*, 5577–5584.
[10] a) R. F. Kelley, W. S. Shin, B. Rybtchinski, L. E. Sinks, M. R. Wasielewski, *J. Am. Chem. Soc.* **2007**, *129*, 3173–3181; b) C.-C. You, F. Würthner, *J. Am. Chem. Soc.* **2003**, *125*, 9716–9725.
[11] F. Würthner, V. Stepanenko, Z. Chen, C. R. Saha-Möller, N. Kocher, D. Stalke, *J. Org. Chem.* **2004**, *69*, 7933–7939.
[12] a) R. K. Dubey, A. Efimov, H. Lemmetyinen, *Chem. Mater.* **2011**, *23*, 778–788; b) N. V. Handa, K. D. Mendoza, L. D. Shirtcliff, *Org. Lett.* **2011**, *13*, 4724–4727; c) S. Dey, A. Efimov, H. Lemmetyinen, *Eur. J. Org. Chem.* **2012**, 2367–2374; d) G. Goretzki, E. S. Davies, S. P. Argent, J. E. Warren, A. J. Blake, N. R. Champness, *Inorg. Chem.* **2009**, *48*, 10264–10274.
[13] A. S. Lukas, Y. Zhao, S. E. Miller, M. R. Wasielewski, *J. Phys. Chem. B* **2002**, *106*, 1299–1306.
[14] a) B. Rybtchinski, L. E. Sinks, M. R. Wasielewski, *J. Am. Chem. Soc.* **2004**, *126*, 12268–12269; b) A. Perez-Velasco, V. Gorteau, S. Matile, *Angew. Chem.* **2008**, *120*, 935–937; *Angew. Chem. Int. Ed.* **2008**, *47*, 921–923; c) C. Hippius, F. Schlosser, M. O. Vysotsky, V. Böhmer, F. Würthner, *J. Am. Chem. Soc.* **2006**, *128*, 3870–3871; d) J. M. Giaimo, A. V. Gusev, M. R. Wasielewski, *J. Am. Chem. Soc.* **2002**, *124*, 8530–8531; e) Y. Shibano, H. Imahori, C. Adachi, *J. Phys. Chem. C* **2009**, *113*, 15454–15466.
[15] a) M. Berberich, A. Krause, M. Orlandi, F. Scandola, F. Würthner, *Angew. Chem.* **2008**, *120*, 6718–6721; *Angew. Chem. Int. Ed.* **2008**, *47*, 6616–6619; b) F. Menacher, H.-A. Wagenknecht, *Eur. J. Org. Chem.* **2011**, 4564–4570.
[16] a) D. M. Guldi, C. Luo, M. Prato, A. Troisi, F. Zerbetto, M. Scheloske, E. Dietel, W. Bauer, A. Hirsch, *J. Am. Chem. Soc.* **2001**, *123*, 9166–9167; b) M. N. Paddon-Row, *Acc. Chem. Res.* **1994**, *27*, 18–25; c) D. Gust, T. A. Moore, A. L. Moore, *Acc. Chem. Res.* **1993**, *26*, 198–205.

[17] Y. Shibano, T. Umeyama, Y. Matano, N. V. Tkachenko, H. Lemmetyinen, Y. Araki, O. Ito, H. Imahori, *J. Phys. Chem. C* **2007**, *111*, 6133–6142.<
[18] C. Bingel, *Chem. Ber.* **1993**, *126*, 1957–1959.
[19] a) N. Armaroli, G. Marconi, L. Echegoyen, J. P. Bourgeois, F. Diederich, *Chem. Eur. J.* **2000**, *6*, 1629–1645; b) T. M. Figueira-Duarte, V. Lloveras, J. Vidal-Gancedo, B. Delavaux-Nicot, C. Duhayon, J. Veciana, C. Rovira, J. F. Nierengarten, *Eur. J. Org. Chem.* **2009**, 5779–5787.
[20] M. E. El-Khouly, O. Ito, P. M. Smith, F. D'Souza, *J. Photochem. Photobiol. C* **2004**, *5*, 79–104.
[21] a) T. J. Kesti, N. V. Tkachenko, V. Vehmanen, H. Yamada, H. Imahori, S. Fukuzumi, H. Lemmetyinen, *J. Am. Chem. Soc.* **2002**, *124*, 8067–8077; b) N. V. Tkachenko, L. Rantala, A. Y. Tauber, J. Helaja, P. H. Hynninen, H. Lemmetyinen, *J. Am. Chem. Soc.* **1999**, *121*, 9378–9387.
[22] W. E. Ford, P. V. Kamat, *J. Phys. Chem.* **1987**, *91*, 6373–6380.
[23] U. Hahn, J. F. Nierengarten, B. Delavaux-Nicot, F. Monti, C. Chiorboli, N. Armaroli, *New J. Chem.* **2011**, *35*, 2234–2244.
[24] V. Chukharev, N. V. Tkachenko, A. Efimov, D. M. Guldi, A. Hirsch, M. Scheloske, H. Lemmetyinen, *J. Phys. Chem. B* **2004**, *108*, 16377–16385.
[25] a) J. Wagger, U. Groselj, A. Meden, J. Svete, B. Slanovnik, *Tetrahedron* **2008**, *64*, 2801–2815; b) B. G. Donner, *Tetrahedron Lett.* **1995**, *36*, 1223–1226; c) A. H. Al-Subi, M. Niemi, J. Ranta, N. V. Tkachenko, H. Lemmetyinen, *Chem. Phys. Lett.* **2012**, *531*, 164–168.
[26] a) D. I. Kreller, P. V. Kamat, *J. Phys. Chem.* **1991**, *95*, 4406–4410; b) Z. Chen, U. Baumeister, C. Tschierske, F. Würthner, *Chem. Eur. J.* **2007**, *13*, 450–465.
[27] M. Niemi, N. V. Tkachenko, A. Efimov, H. Lehtivuori, K. Ohkubo, S. Fukuzumi, H. Lemmetyinen, *J. Phys. Chem. A* **2008**, *112*, 6884–6892.
[28] V. Vehmanen, N. V. Tkachenko, H. Imahori, S. Fukuzumi, H. Lemmetyinen, *Spectrochim. Acta Part A* **2001**, *57*, 2229–2244.

Received: September 21, 2012
Revised: February 1, 2013
Published online: ■■ ▮▮, 0000

Perylene diimide based donor–acceptor system: New bay-functionalized derivatives of 1,7- and 1,6-regioisomers of dipyrrolidinyl-substituted perylene diimide have been synthesized (see figure) and covalently linked with C_{60}. Efficient photoinduced electron transfer from the perylene diimide chromophore to C_{60} has been shown, which occurs in both polar and nonpolar environments. Differences in the chemical behavior and photodynamics of the two regioisomers have been exposed.

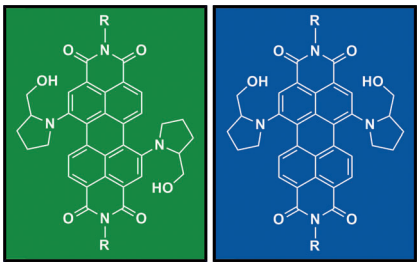

Regioisomeric PDI dyes

R. K. Dubey, M. Niemi, K. Kaunisto, A. Efimov, N. V. Tkachenko, H. Lemmetyinen* ..... ▮▮▮▮–▮▮▮▮

Direct Evidence of Significantly Different Chemical Behavior and Excited-State Dynamics of 1,7- and 1,6-Regioisomers of Pyrrolidinyl-Substituted Perylene Diimide